



**SYNTHESIS, OPTICAL AND SEMICONDUCTOR
CHARACTERIZATION OF MOLYBDENUM DISELENIDE
(MoSe₂) THIN FILMS**

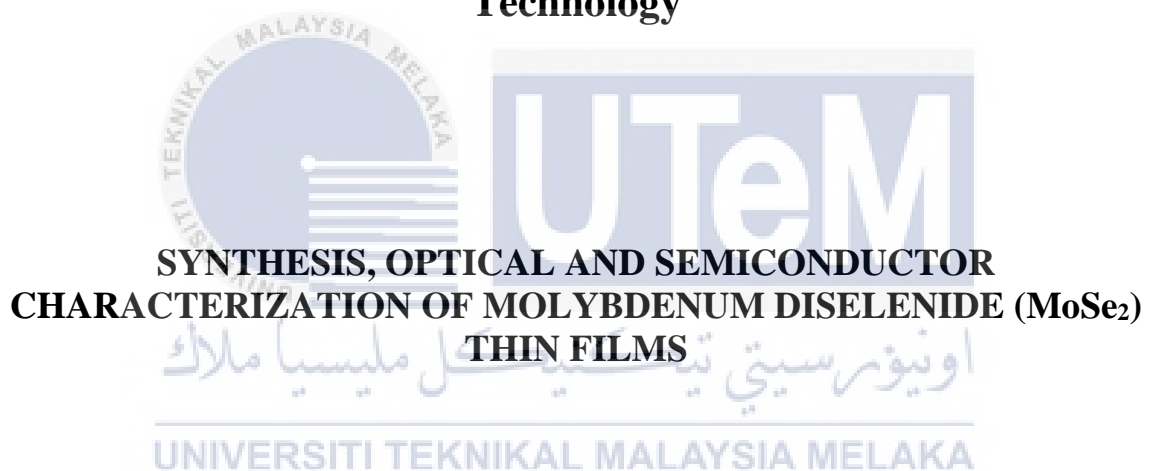
LIM THIAN MEE
اونيورسيتي تيكنيكل مليسيا ملاك
UNIVERSITI TEKNIKAL MALAYSIA MELAKA

**BACHELOR OF MANUFACTURING ENGINEERING
TECHNOLOGY (PRODUCT DESIGN) WITH HONOURS**

2023



**Faculty of Mechanical and Manufacturing Engineering
Technology**



Lim Thian Mee

Bachelor of Manufacturing Engineering Technology (Product Design) with Honours

2023

**SYNTHESIS, OPTICAL AND SEMICONDUCTOR CHARACTERIZATION OF
MOLYBDENUM DISELENIDE (MoSe₂) THIN FILMS**

LIM THIAN MEE

**A thesis submitted
in fulfillment of the requirements for the degree of
Bachelor of Manufacturing Engineering Technology (Product Design) with Honours**



UNIVERSITI TEKNIKAL MALAYSIA MELAKA

2023

DECLARATION

I declare that this final year project entitled “Synthesis, Optical and Semiconductor characterization of Molybdenum diselenide (MoSe₂) thin films” is the result of my own research except as cited in the references. The final year project has not been accepted for any degree and is not concurrently submitted in candidature of any other degree.

Signature

:



Name

:

Lim Tian Mee

Date

:

19 January 2023



اونيورسيتي تيكنيكل مليسيا ملاك

UNIVERSITI TEKNIKAL MALAYSIA MELAKA

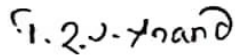
APPROVAL

I hereby declare that I have checked this thesis and in my opinion, this thesis is adequate in terms of scope and quality for the award of the Bachelor of Manufacturing Engineering Technology (Product Design) with Honours.

PROF. TS. DR. T. JOSEPH SAHAYA ANAND

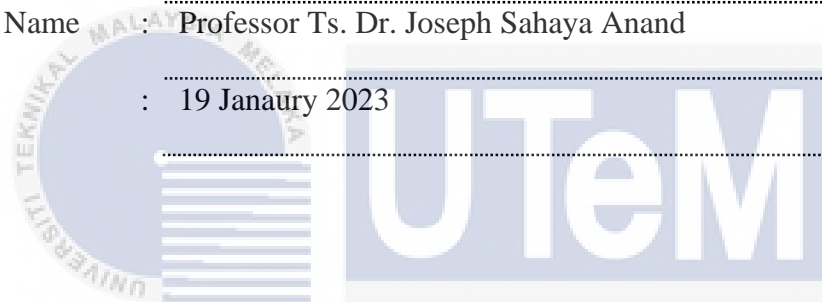
Professor

Faculty of Mechanical & Manufacturing
Engineering Technology
Universiti Teknikal Malaysia Melaka

Signature : 

Supervisor Name : Professor Ts. Dr. Joseph Sahaya Anand

Date : 19 January 2023



اونيورسيتي تيكنيكل مليسيا ملاك

UNIVERSITI TEKNIKAL MALAYSIA MELAKA

DEDICATION

I dedicate this thesis to my beloved parents which is my father, Lim Ah Chui and my mother, Tay Ley Ha, who have been a constant source of inspiration and encouragement have taught me to work hard for the things that I aspire to achieve. To my supervisor who guided and helped us in this process and the committee who kept us on track. Thank you for the guidance, knowledge, understanding, and skills that has been the source of my strength throughout this project.



ABSTRACT

Both efficient and more economical semiconductor thin film materials are of current interest which is growing day by the day, especially with the advancement of nanotechnology and polymer science. Despite the fact that silicon solar cells now dominate the PV market, thin film-based technologies have nearly equaled their performance and yet have space for improvement. The low availability of several components in current commercially accessible PV technologies, as well as the recent high cost of silicon modules, has drawn the scientific community's attention to cost-effective materials. Due to their exceptional structural, optical and electrical properties, layered transition chalcogenide materials such as Molybdenum diselenide (MoSe_2) have attracted a lot of attention recently. Electrodeposition, as a well-established chemical method with intrinsic large-scale manufacturing capabilities, be used to build low-cost solar cells with direct band gaps and the ability to control the band gap through in-situ doping for the creation of possible hereojunctions. Electrochemical techniques were used to investigate the electrodeposition of Molybdenum diselenide (MoSe_2) thin films on an Indium Tin Oxide (ITO) coated glass substrate. The cyclic voltammetry method was used to determine the optimal potential for MoSe_2 thin deposition, and the thickness was investigated using the weight gain method. X-ray diffraction (XRD) will confirm the structural characterization and crystallographic nature of these films, while scanning electron microscopy (SEM) will reveal information about their grain or molecular structures by analysing their surface morphology. A UV-Vis-NIR Spectrophotometer was used to investigate the thin films' optical characteristics. Optical absorption can be investigated to determine the band gap nature of these kind of materials. Their stoichiometric relationships will be determined by compositional analysis using Energy dispersive X-ray analysis (EDX). The semiconductor properties of these materials, such as doping density, band bending, and valence band edge, are determined using the Mott-Schottky plot. These characteristics are the deciding factors for photoelectrochemical solar cells, and they are used to determine the conversion efficiency of these materials.

ABSTRAK

Kedua-dua bahan filem nipis semikonduktor yang cekap dan lebih ekonomik adalah minat semasa yang berkembang dari hari ke hari, terutamanya dengan kemajuan teknologi nano dan sains polimer. Walaupun sel suria silikon kini menguasai pasaran PV, teknologi berasaskan filem nipis telah hampir menyamai prestasi mereka dan masih mempunyai ruang untuk penambahbaikan. Ketersediaan rendah beberapa komponen dalam teknologi PV semasa yang boleh diakses secara komersil, serta kos modul silikon yang tinggi baru-baru ini, telah menarik perhatian komuniti saintifik kepada bahan yang kos efektif. Disebabkan oleh sifat struktur, optik dan elektriknya yang luar biasa, bahan chalcogenide peralihan berlapis seperti Molibdenum diselenide (MoSe_2) telah menarik banyak perhatian baru-baru ini. Electrodeposition, sebagai kaedah kimia yang mantap dengan keupayaan pengilangan berskala besar intrinsik, digunakan untuk membina sel suria kos rendah dengan jurang jalur langsung dan keupayaan untuk mengawal jurang jalur melalui doping in-situ untuk penciptaan kemungkinan sambungan sini. Teknik elektrokimia digunakan untuk menyiasat elektrodeposisi filem nipis Molibdenum diselenide (MoSe_2) pada substrat kaca bersalut Indium Tin Oxide (ITO). Kaedah voltametri kitaran digunakan untuk menentukan potensi optimum bagi pemendapan nipis MoSe_2 , dan ketebalan disiasat menggunakan kaedah penambahan berat. Pembelauan sinar-X (XRD) akan mengesahkan pencirian struktur dan sifat kristalografi filem ini, manakala mikroskop elektron pengimbasan (SEM) akan mendedahkan maklumat tentang struktur bijian atau molekulnya dengan menganalisis morfologi permukaannya. Spektrofotometer UV-Vis-NIR digunakan untuk menyiasat ciri optik filem nipis. Penyerapan optik boleh disiasat untuk menentukan sifat jurang jalur bahan jenis ini. Hubungan stoikiometrinya akan ditentukan oleh analisis komposisi menggunakan analisis sinar-X penyebaran tenaga (EDX). Sifat semikonduktor bahan ini, seperti ketumpatan doping, lenturan jalur, dan tepi jalur valens, ditentukan menggunakan plot Mott-Schottky. Ciri-ciri ini adalah faktor penentu untuk sel suria fotoelektrokimia, dan ia digunakan untuk menentukan kecekapan penukaran bahan-bahan ini.

ACKNOWLEDGEMENTS

First and foremost, I would like to extend my appreciation to the Universiti Teknikal Malaysia Melaka (UTeM) for providing the research platform. Thank you also to the Perbadanan Tabung Pendidikan Tinggi Nasional (PTPTN) for the financial assistance.

My utmost appreciation goes to my supervisor, Prof. Ts. Dr. Joseph Sahaya Anand, Universiti Teknikal Malaysia Melaka (UTeM) who constantly supported my journey with all his support, help, advice and inspiration. His constant patience for guiding and providing priceless insights will forever be remembered.

Last but not least, from the bottom of my heart a gratitude to my beloved family for their endless support, love and prayers and thank for their encouragements and who have been the pillar of strength in all my endeavors. My eternal love also to all my relatives and classmates, for their patience and understanding. Finally, thank you to all the individual(s) who had provided me the assistance, support and inspiration to accomplish on my study.

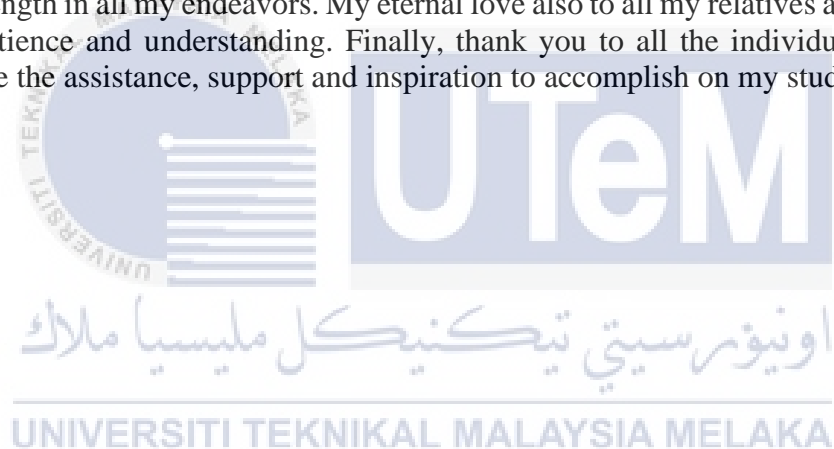


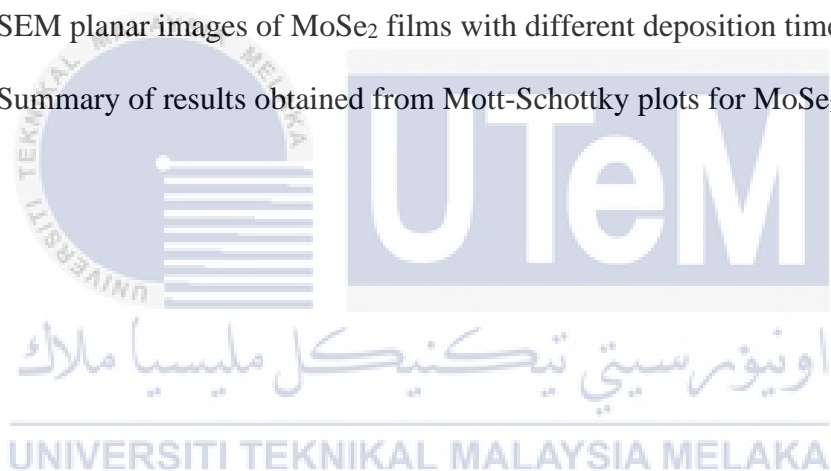
TABLE OF CONTENTS

	PAGE
DECLARATION	
APPROVAL	
DEDICATION	
ABSTRACT	i
ABSTRAK	ii
ACKNOWLEDGEMENTS	iii
TABLE OF CONTENTS	iv
LIST OF TABLES	vi
LIST OF FIGURES	vii
LIST OF SYMBOLS AND ABBREVIATIONS	ix
LIST OF APPENDICES	xii
CHAPTER 1 INTRODUCTION	1
1.1 Background	1
1.2 Problem Statement	4
1.3 Research Objective	5
1.4 Scope of Research	5
1.5 Project Outline	6
CHAPTER 2 LITERATURE REVIEW	8
2.1 Introduction	8
2.2 Transition Metal Chalcogenide	8
2.2.1 Molybdenum diselenide, MoSe ₂	10
2.3 Compound Semiconductor	12
2.4 Thin film	14
2.4.1 Thin Film Growth	17
2.4.2 Growth Modes of Thin Film	18
2.5 Cyclic Voltammetry (CV)	19
2.6 Thin Film Deposition Method	21
2.6.1 Electrodeposition	22
2.6.2 Chemical Vapour Deposition (CVD)	24
2.7 X-Ray Diffraction (XRD)	25
2.8 Scanning Electron Microscope (SEM)	27
2.8.1 Scanning Electron Microscopy (SEM) Based Energy Dispersive X-ray Spectroscopy (EDX)	30

2.9	Optical properties by Ultraviolet-Visible-Near Infrared (UV/Vis/NIR) Spectrophotometer	30
2.10	Photoelectrochemical Studies	34
2.11	Summary or Research gap	38
CHAPTER 3 METHODOLOGY		40
3.1	Introduction	40
3.2	Substrate Preparation	42
3.3	Synthesis of MoSe ₂ thin film	42
3.4	Film Thickness Measurement	43
3.5	Structural Studies by X-ray Diffraction (XRD)	44
3.6	Surface Morphological Studies by Scanning Electron Microscope (SEM)	44
3.7	Optical Studies by UV/Vis/NIR Spectrophotometer	45
3.8	Semiconductor Parameter by Mott-Schottky Plot	46
CHAPTER 4 RESULTS AND DISCUSSION		48
4.1	Introduction	48
4.2	Film Thickness Measurement	49
4.3	XRD Structural Analysis	50
4.4	SEM Surface Morphological Analysis	53
4.5	Optical Analysis	55
4.6	Mott-Schottky Analysis	57
CHAPTER 5 CONCLUSION AND RECOMMENDATIONS		60
5.1	Conclusion	60
5.2	Recommendations	61
5.3	Project Potential	62
REFERENCES		64
APPENDICES		74

LIST OF TABLES

TABLE	TITLE	PAGE
Table 2.1	Comparison between materials that used in solar cells application	16
Table 2.2	Flat band potential for thin films of NiSSe (S.Shariza & Anand, 2018)	37
Table 4.1	Thickness of MoSe ₂ thin films	49
Table 4.2	XRD comparison of standard JCPDS values with experimental MoSe ₂ values	51
Table 4.3	SEM planar images of MoSe ₂ films with different deposition times	54
Table 4.4	Summary of results obtained from Mott-Schottky plots for MoSe ₂	59



LIST OF FIGURES

FIGURE	TITLE	PAGE
Figure 2.1	Position of transition metals in periodic table (A. Brent Young, 2006)	9
Figure 2.2	The growth models of thin film (Hideaki Adachi & Kiyotaka Wasa, 2012)	17
Figure 2.3	(a) Layer-by-layer growth mode (b) Island growth mode (c) Layer-plus-island growth mode (T. Devillers, 2008)	18
Figure 2.4	Cyclic voltammetry (Ying Zhuo, 2021)	21
Figure 2.5	Electrodeposition setup (Ayotunde Adigun Ojo & Imyhamy Mudi Dharmadasa, 2018)	23
Figure 2.6	Aspects of a CVD process (Akhtar, M., 2013)	24
Figure 2.7	X-rays diffraction technique (Nutan S. Satpute & S.J. Dhoble, 2021)	26
Figure 2.8	(a) XRD pattern of an amorphous material and (b) crystalline material (Lamas, D.G., 2017)	27
Figure 2.9	Components of Scanning Electron Microscope (SEM) (Dr. Tapanendu Kamilya, 2020)	28
Figure 2.10	SEM images of CdTe thin films in surface morphology and cross-section view (Rahman Kazi Sajedur, 2019)	29
Figure 2.11	EDX result on CdSe thin film (Erat <i>et. al</i> , 2008)	30
Figure 2.12	Band diagram of semiconductor for (a) direct band gap and (b) indirect band gap (Amelia Carolina Sparavigna, 2014)	33
Figure 2.13	$(\alpha h\nu)^2$ plots with respect of photon energy $(h\nu)$ for CdTe/CdS thin film (K. N. Nithyayini & Sheela K. Ramasesha, 2015)	34

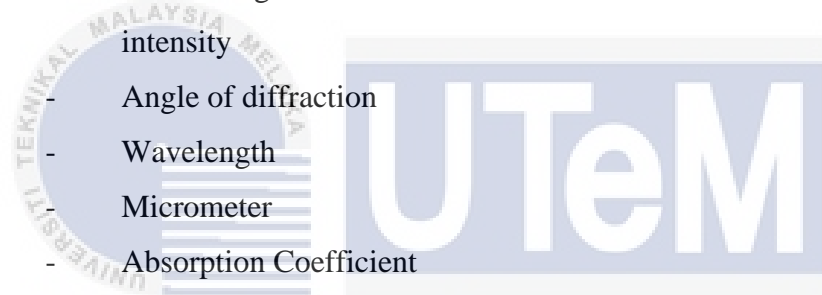
Figure 2.14 Mott-Schottky plot of NiSSe thin film (S.Shariza & Anand, 2018)	37
Figure 2.15 Mott-Schottky plot of NiS ₂ thin film (Anand, 2013)	38
Figure 3.1 Flow chart of this project	41
Figure 3.2 Electrolytic cell setup of MoSe ₂ thin film deposition	43
Figure 3.3 X-ray diffractometer XPERT PROMPD PW 3040/60 (Mohd Shahrulrizan Bin Ibrahim, 2021)	44
Figure 3.4 JSM-6400 JEOL Scanning Electron Microscope (SEM) (ebay, 2022)	45
Figure 3.5 UV-Vis-NIR Spectrophotometer (EVISA, 2003)	46
Figure 4.1 Thickness of MoSe ₂ thin film with deposition time	50
Figure 4.2 XRD pattern of MoSe ₂ thin film at different deposition times	52
Figure 4.3 Graph of $(\alpha h\nu)^2$ versus photon energy (hν) with different deposition times	56
Figure 4.4 Graph of bandgap versus deposition time	57
Figure 4.5 Mott-Schottky plot for MoSe ₂ thin films at different deposition time	58

LIST OF SYMBOLS AND ABBREVIATIONS

α -silicon	-	Amorphous silicon
CdS	-	Cadmium Sulphide
CdSe	-	Cadmium Selenide
CdTe	-	Cadmium Telluride
CIGS	-	Copper Indium Gallium Selenides
CV	-	Cyclic voltammetry
CVD	-	Chemical vapour deposition
Cu	-	Copper
EDX	-	Energy Dispersion X-ray Spectroscopy
HCl	-	Hydrochloric acid
ITO	-	Indium Tin Oxide
JCPDS	-	Joint Committee on Powder Diffraction Standards
MBE	-	Molecular Beam Epitaxy
Mn	-	Manganese
MoSe ₂	-	Molybdenum diselenide
PEC	-	Photoelectrochemical cell
PSM	-	Projek Sarjana Muda
PV	-	Photovoltaic
PVD	-	Physical Vapor Deposition
SCE	-	Saturated Calomel Electrode
Se	-	Selenide
SEM	-	Scanning Electron Microscope
Si	-	Silicon
TMCs	-	Transition Metal Chalcogenides
TMDs	-	Transition Metal Dichalcogenides
UV-Vis- NIR	-	Ultraviolet-Visible-Near Infrared
W	-	Tungsten
XRD	-	X-ray Diffraction

%	-	Percentage
ϵ_0	-	Free space permittivity (8.854×10^{-12} F/m)
ϵ_S	-	Semiconductor dielectric constant
η_{\max}	-	Maximum coefficient
Å	-	Angstrom
A	-	Area of contact
C	-	Capacitance
c	-	Speed of light (3×10^8 m/s)
cm	-	Centimeter
cm ²	-	Centimeter square
cm ³	-	Centimeter cube
cos	-	cosine
C_{SC}^2	-	Space charge capacitance
d	-	Thickness of the crystal
e	-	Dielectric constant
E	-	Photon energy
E_c	-	Conduction band edge
E_g	-	Energy gap
eV	-	Electron volt
E_v	-	Valence band edge
g	-	Gram
h	-	Plank's constant (6.63×10^{-34} J/S)
k_B	-	Boltzmann's constant (1.38×10^{-23} J/K)
keV	-	Kilo electron volt
m	-	Meter
M	-	Molarity
m ²	-	Meter square
ml	-	Milliliter
mm	-	Millimeter
N	-	Charge carrier concentration
n	-	Transition probability, n = 0.5, 1.5, 2 and 3

N_c	-	Conduction band
N_D	-	Doping density
nm	-	Nanometer
°	-	Degree
°C	-	Degree Celsius
T	-	Temperature
V	-	Volt
V_b	-	Band bending
V_{FB}	-	Flat band potential
W	-	Depletion layer width
β	-	Broadening of diffraction line measured at half of its maximum intensity
θ	-	Angle of diffraction
λ	-	Wavelength
μm	-	Micrometer
α	-	Absorption Coefficient



اونيورسيتي تيكنيكل مليسيا ملاك
 UNIVERSITI TEKNIKAL MALAYSIA MELAKA

LIST OF APPENDICES

APPENDIX	TITLE	PAGE
APPENDIX A	Gantt Chart for PSM 1 (Semester 6, March, 2022)	74
APPENDIX B	Gantt Chart for PSM 2 (Semester 8, October, 2022)	75



CHAPTER 1

INTRODUCTION

1.1 Background

In recent years, semiconducting thin film solar cells have gained lots of interest as a second-generation renewable clean energy source to replace traditional energy sources such as coal and petroleum. Recently, the bulk of solar cells have been made of silicon, either monocrystalline or large-grained polycrystalline. Silicon, an elemental semiconductor, as it has possesses a very well combination of electrical, chemical and physical properties, as well as good stability, making it the best material for microelectronics, specifically devices based on solar energy. Futhermore, silicon's commercial value in the photoelectrochemical sector has increased as a result of its application in electronics. However, due to the scarcity and high cost of silicon, cost reduction becomes a critical problem that may be addressed by concentrating on new silicon alternative materials and improving the manufacturing process. Semiconducting materials are cheap and plentiful on Earth. The use of these materials in solar cells for this purpose is still more cheaper than photovoltaic technology based on silicon (Rahaman, M.Z. & Akther Hossain, A.K.M, 2018). Thus, finding innovative materials with optimal properties for electrochemical energy conversion is the main focus for electrochemical photovoltaic technology.

Among the many other transition metal chalcogenides (TMCs), metal dichalcogenides MX_2 ($\text{X}=\text{S}$, Se , and Te), are semiconductors that can be used as an efficient photovoltaic material. Since they have good electrical and optical properties, metal chalcogenides have gained increased popularity as a suitable solar absorber material. Hence,

an exploration of minimum cost and earth-abundant absorber materials of metal dichalcogenides MX_2 ($X=S, Se, \text{ and } Te$) for high-efficiency solar cells is very important and popular (Anand *et al.*, 2013). It provides band gap of 1-3eV that match with solar spectrum as well as a larger optical absorption band gap and semiconducting properties. Therefore, in this research, Molybdenum deselenide ($MoSe_2$) that is a new ternary transition metal dichalcogenide was study.

A two-dimensional pattern of periodicity named "thin film" exists in every solid or liquid system. Thin films' characteristics generally differ greatly from bulk materials because of surface and interface effects, which can influence behavioural pattern. Several research studies have been conducted to discover thin film material for use in solar cells. The best semiconducting materials for direct conversion of light to electrical energy applications are bulk or thin film materials with a low band gap of 1-2 eV. In terms of thickness, films are divided into two categories: thick film and thin film. Thin films are thin layers of deposited material on a substance with thicknesses ranging from tenths of a nanometer (nm) to 1 micrometre (μm) with bulk characteristics that differ. Aluminium thin film, for example, has 5 times the strength of iron in bulk because to its layer-by-layer crystallography. When compared to thin film, thick film is typically used for weld bases and has a thickness of 1-5 μm , whereas foil has a thickness of more than 5 μm and does not require any support such as a substrate or base material.

Electrodeposition, a well-known chemical technique, can be used to create thin films. The electrodeposition method for preparing thin film of transition metal chalcogenide is gaining popularity since it is very cheap, simple, and practical for wide range of applications. Electrodeposition is a thin film and/or powder preparation process that uses an external current source to perform reduction or oxidation reactions. Electrodeposition method is

chosen for this research which is chemical vapour deposition (CVD) methods to deposit the thin film. At room temperature, the CVD process could produce high quality and good adhesive coatings on metal or nonmetal substrates such as metal substrates or Indium Tin Oxide (ITO) glass substrates. Thin films are typically deposited using the CVD technique, which is influenced by the economic, simplicity, and wide scale of the deposition rate, as well as the environmentally friendly process (Murai *et al.*, 2016). For use in photovoltaic cells, the electrodeposition process allows for simple changes in optical properties (band gap) and structure (lattice constant) by modulating bath parameters such as applied potential, bath temperature and pH. As a result, the electrodeposition process deserves a place in the future for large-scale commercialization of numerous new photovoltaic applications and devices that are less expensive than their silicon counterparts.

Futhermore, solar panels are an optoelectronic device that is used and is becoming increasingly important in today's industry as a source of energy in everyday life consumption. Solar panels are photovoltaic solar powered boards that use daylight as a source of energy to generate electricity. A photovoltaic (PV) module is a bundled, linked grouping of photovoltaic solar cells that are typically 6×10 in size. Photovoltaic modules are the photovoltaic exhibit of a photovoltaic framework that generates and stores solar-powered energy in residential and business applications. Solar powered water heating systems are the most well-known application of solar-based energy gathering outside of horticulture. Since 2012, the cost of solar-based electrical power has continued to decrease, and in many countries, it has been less expensive than normal petroleum derived power from the power network.

This present research focuses on the optical and semiconductor properties on Molybdenum diselenide (MoSe_2) thin film and the use of chalcogenide to increase the

conversion efficiency in solar cells as well as reduce the cost to produce new thin film for solar panel.

1.2 Problem Statement

As discussed in earlier section, the objectives of this study is to find alternative substances for solar energy conversion. With the performance limiting factors of these photoabsorbers, increased the concern together with suggestions from this study for further improvement. Solar energy is a renewable energy source which provides the world's most abundant, safe, and environmentally friendly energy. Aside from that, thin film solar cells have recently become the most interesting topic in solar cell research and development as an energy conversion technology. Solar cells can absorb photons from the light spectrum and convert them to electrical energy. Solar energy, on the other hand, has been prevented from becoming a more widely used energy source due to the problems such as its high cost and inconsistent availability.

Due to its high stability and well-balanced combination of electron, physical, and chemical properties, silicon is a well-known material for solar cells (Hao *et al.*, 2015). Despite the fact that silicon is a widely used material, it is still a costly material in pure silicon wafers, which might need complex alignment and design throughout the production process. In order to compete with other photovoltaic (PV) technologies, silicon material conversion efficiency is only 12-14 %, however small area (1cm^2) of silicon based thin films for solar panels have conversion efficiency up to 20% (Isabella et al, 2014). However, other materials with cheap cost, simplicity of production, great visible light absorption, and acceptable semiconducting parameters are being developed to replace silicon as a solar cell material.

Transition metal dichalcogenides (TMDs) thin films, such as Tungsten diselenide (WSe₂) and Molybdenum disulfide (MoS₂), have recently been found as a material for use in solar cells. TMDs thin films have strong optical and semiconducting characteristics, making them suitable for use as a photovoltaic (PV) material. TMDs thin films can be produced using a low-cost, relatively simple electro-deposition process, which is chemical vapour deposition techniques (CVD).

In this study, Molybdenum diselenide (MoSe₂) thin film, a transition metal dichalcogenides (TMDs) material, would be produced using a simple and low-cost electrodeposition process to replace existing silicon thin film for solar cell applications.

1.3 Research Objective

In this project, the objectives that are achieved in the research are as follows:

- a) To synthesis stoichiometric Molybdenum diselenide (MoSe₂) thin films by using electrodeposition.
- b) To analyse the optical characterization of Molybdenum diselenide (MoSe₂) thin films by using UV-Vis-NIR spectrophotometer.
- c) To determine semiconductor parameters of Molybdenum diselenide (MoSe₂) thin films for photoelectrochemical solar cells by using Mott-Schottky Plot.

1.4 Scope of Research

The following are the scope of this research:

- The properties of Molybdenum diselenide (MoSe₂) thin films for use in photochemical (PEC) solar cells.
- The synthesis of thin films of Molybdenum diselenide (MoSe₂) would be done in chemical vapour deposition technique from high purity materials.

- X-rays Diffraction (XRD) to determine structural properties of Molybdenum diselenide (MoSe_2) thin films.
- Scanning Electron Microscope (SEM) to examine the morphological properties of Molybdenum diselenide (MoSe_2) thin films.
- Optical characterization analysis by UV-Vis-NIR spectrophotometer for the band gap nature of Molybdenum diselenide (MoSe_2) thin films.
- The semiconductor parameters of Molybdenum diselenide (MoSe_2) thin films are derived from the Mott-Schottky plot.

1.5 Project Outline

This PSM report is classified into three main chapters, which is introduction, literature review, methodology, result and discussion and conclusion and recommendations.

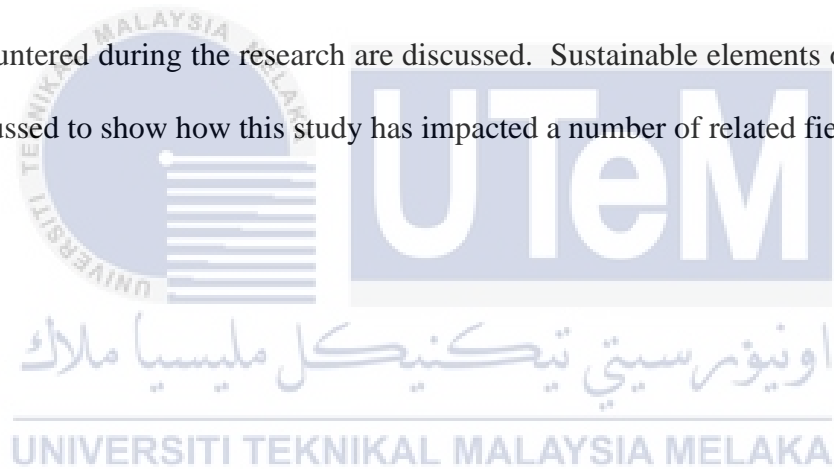
Chapter 1 of the project is an introduction. It examines the research background. Problems are identified through research, experiment and observation by using data and instrument. This is followed by objectives to be achieved throughout the study, scope of project, and also the project outline. Each of these sections can help in the understanding of the project.

Chapter 2 of the project is literature review. This part covered information that was linked to this research's title and the previous studies has already been published. This chapter can help with research and provide an overview of the relevant title. Other researchers' investigations provided a clear background for the research, and improvements could be made based on their previous work.

Chapter 3 of the project is methodology of the research. The methodologies used in the research have been discussed in this part. This chapter discussed the research method, the material use and the characterization of the material's method included in the research.

Chapter 4 of the project is result and discussion of the research. Data obtained using the procedures outlined in the previous chapter is analysed. The analysed data is used to provide a brief summary and explanation. This chapter includes some technical opinions and professional views to enrich the collected outcomes and support the discussion.

Chapter 5 of the project is conclusion and recommendations of the research. The conclusions make a clear statement based on the objectives. Recommendations for resolving issues encountered during the research are discussed. Sustainable elements of the research is also discussed to show how this study has impacted a number of related fields.



CHAPTER 2

LITERATURE REVIEW

2.1 Introduction

In recent year, thin film production has been highlighted as a major strategy to solve growing challenges in solar cell, corrosion resistant coating, microelectronics, optical, magnetic, laser, and gas sensor devices due to semiconductor material properties. Transition metal chalcogenides, a series of semiconductor materials that can be used in various applications from antibacterial particles to thin films in energy conversion devices, are interesting choices for photovoltaic conversion. Simply, this application is a branch of technology that involves the production of solar energy using solar cells. The thickness of these thin films ranges from a few nanometers to hundreds of micrometers, and their structural, physical and chemical properties are closely related to the production technique. A wide range of electrochemical, chemical and physical deposition method enable the production of low-cost of transition metal chalcogenide on large region of the desired structure and geometry. For analyzing the optical absorption of thin film, it is necessary to develop the band gap nature of these materials in terms of levels of energy between the valence bands and conduction bands that occurs in the thin film.

2.2 Transition Metal Chalcogenide

Transition Metal Chalcogenide (TMCs) is the combination of the transition metal and chalcogenide. Figure 2.1 shown Periodic table of transition metal chalcogenide in group 16 are known as chalcogens . The name chalcogenide is more usually applied to sulphides, selenides, and tellurides rather than the oxides. The transition metal is a periodic table

element which belongs to the d-block. The transition metal belongs to the periodic table's groups 3 to 12. Tungsten (W), Manganese (Mn), and Copper (Cu) are examples of transition metals.

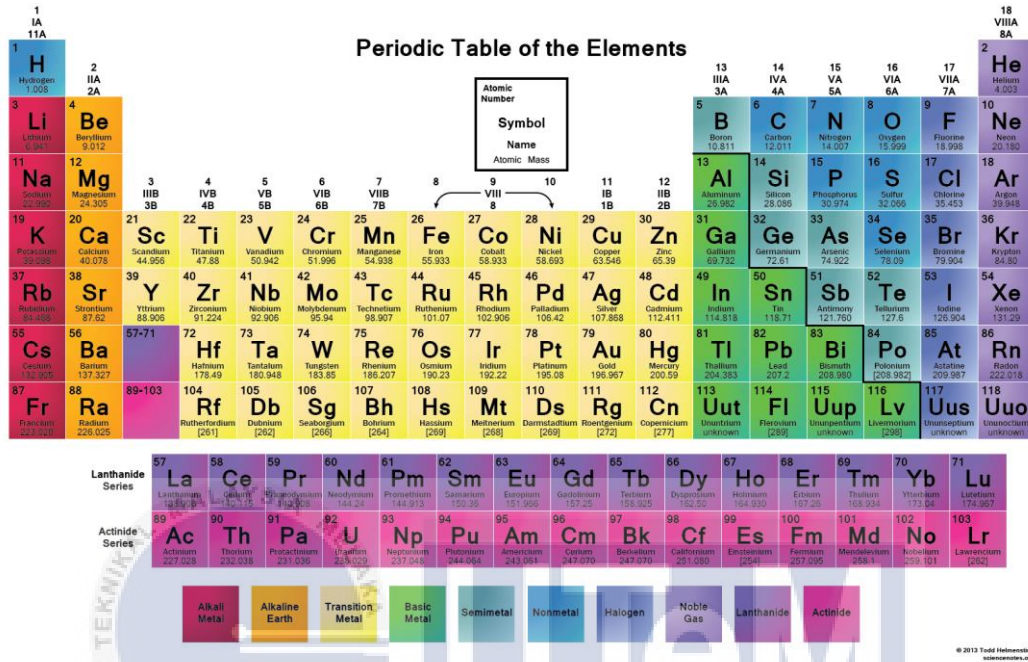


Figure 2.1 Position of transition metals in periodic table (A. Brent Young, 2006)

TMCs are semiconductors with a layered structure (Martin-Litas *et al.*, 2002). When one, two, or three types of chalcogenide elements are used as a combination with the transition metal, the TMCs are classed as binary, ternary, or quaternary transition metal chalcogenide. TMCs have attracted attention over recent years due to their interesting structural chemistry, unique electrical characteristics, and rich intercalation chemistry (Tremel *et al.*, 1995).

TMCs have been the target of several studies for their thin film characteristics. This is mostly due to the fact that many applications required the thin layers of TMCs on substrates (Anand & Shariza, 2012). These studies were conducted on a variety of TMCs, including binary, ternary, and quaternary types of TMCs.

Solar cells, solar selective coatings, photodiode arrays, sensors, photoconductors and other applications are possible using TMCs thin film. Deposition of transition metal chalcogenides can be done using a various methods. Vacuum evaporation, chemical vapour deposition, electrodeposition, electroconversion, chemical bath deposition, and other methods can be used to deposit TMCs thin films (Mane & Lokhande, 2000).

TMCs are a type of semiconducting material that may be used as a photovoltaic material (Anand & Shariza, 2012). This means that TMCs may be used to convert solar or photo energy directly into electrical energy. The capacity of TMCs to absorb light energy is determined by the bandgap energy range in the TMCs. The band gap of the TMCs must be in the region of 1-4eV for visible light to be absorbed by them.

Many studies on ternary chalcogenides materials have been conducted in recent decades. These studies are being carried out to determine whether the ternary chalcogenides materials can be used to replace the existing material used as electrodes in electrochemical photovoltaic cells and then will increase the photovoltaic cells' conversion efficiency. For example, Subramanian *et al.* (2003) had done the studies on the $\text{SnS}_{0.5}\text{Se}_{0.5}$ thin films, Ajalkar *et al.* (2004) had done the research on the $[\text{Mo}(\text{S}_{1-x}\text{Se}_x)_2]$ thin films while Kumar and Dwivedi (2013) had done the studies on the $\text{CdS}_{0.5}\text{Se}_{0.5}$ thin films recently.

2.2.1 Molybdenum diselenide, MoSe₂

Molybdenum dichalcogenides are part of the layered transition metal dichalcogenides family. Molybdenum diselenide, MoSe_2 is combined with molybdenum and selenium. It is made up of sandwiched layers that are weakly coupled, such as Se – Mo – Se, with a Mo atom layer connected between two Se layers (J. A. Wilson, 1969). Six chalcogenide atoms always coordinate the metal atom. The trigonal prismatic and trigonal

antiprismatic (although deformed, it's generally referred to as octahedral.) geometries are the two possible geometries.

The nature of the interlayer bonding forces is van der Waals, leads to significant interlayer distances. MoSe₂ is very anisotropic and has unique structural features as a result of its structure (Ali Hussain and Sushil Auluck, 2005). MoSe₂ is an interesting component of the transition metal dichalcogenides (TMDs) family that has recently attracted a lot of interest for its use in photocatalytic, optoelectronic systems and electrochemical. MoSe₂ is also flexible and has strong carrier mobility, making it a good choice for produce flexible high mobility electrical devices such Schottky barrier devices, solar cells and FETs. Additionally, this material can also be used as a catalyst and is a good lubricant (Th. Boker and R Severin, 2001).

Along with its layered structure, as well as the size and electrical conductivity of Se, MoSe₂ is ideal for supporting counterions in electrochemical energy storage devices such as lithium-ion battery and sodium-ion batteries. In the hydrogen process of evolution (HER) and other electrocatalytic processes (for example, in lithium-oxygen batteries), the unsaturated Se atoms along the edge, as well as those at weak areas or a changed basal plane, exhibit higher electrochemical performance. MoSe₂ is also a perfect choice for photoelectrochemical solar cells and photocatalysis due to its tunable band gap (Kaili Zhang, 2019).

The semiconducting MoX₂ or WX₂ (X= S or Se) indicate tuneable band-gap qualities related to the number of atomic layers (Shan and Heinz, 2010), as well as strong light-matter interactions that manage up to 10% absorption of incident solar illumination in a thickness of less than 1nm, capturing sunlight stronger by an order of magnitude than normal semiconductors (that is, GaAs and Si) (Britnell, 2013).

Furthermore, according to Lu, J. *et al.* (2017), monolayer MoSe₂ has a direct band gap of 1.5 eV, which is near to the ideal value of band gap for solar energy applications which including single-junction solar cells and photoelectrochemical cells. For the greatest theoretical efficiency of a solar cell, this band gap falls between 1.0 eV and 1.6 eV, therefore MoSe₂ is an important potential material to provide an efficient cell. MoSe₂ offers the same long-term durability and stability in power conversion efficiency as other chalcogenide-based cells.

2.3 Compound Semiconductor

Semiconductor materials are found in the periodic table's column IV and adjacent columns. Column IV semiconductors are known as elemental semiconductors since they are made up of only one atom species. A semiconductor is a material that lies between conductors and insulators in terms of electrical current conductivity. A semiconductor is neither a good conductor nor an good insulator in its pure (intrinsic) state.

The electrical conductivity of a semiconductor is influenced by various of parameters, such as the applied voltage or current, as well as the intensity of infrared, ultraviolet, or visible light on the surface. Silicon (Si) is a semiconductor materials that commonly used and relevant to solar cell operation. The most popular semiconductor materials used in solar cells are amorphous silicon (Si), crystalline and polycrystalline. The selection of solar cell materials is generally based on how well their absorption properties fit the solar radiation and their production costs. Silicon is a popular option since its absorption properties are close to those of the solar spectrum, and silicon manufacturing technology has advanced due to its widespread use in the semiconductor devices sector. Despite the availability of numerous alternative technologies, silicon-based PV plants to produce for

more than 90% of newly installed PV plants, and they are estimated to remain the most widely used PV technology (Freiburg, 2022).

The structure of the energy band gap as a function of the wave vector of a semiconductor material are key characteristics crucial to the operation of the solar cell. The number of photons reflected from the solar cell's surface, the semiconductor band-gap energy, which is the lowest amount of light (photon) energy the material absorbs, and the thickness of layer all influence how much sunlight a PV cell absorbs (K. W. Mitchell, Margorie L. Tatro, 2017). The temperature change of the band gap energy and the amplitude of the wave vector associated with low-energy transitions are the major factors of interest. In a semiconductor, electrons receive energy (for example, from ionizing radiation) to be able cross the band gap and enter the conduction band. The band gap is smaller in semiconductors, allowing a valence electron to escape. If it absorbs a photon, it moves into the conduction band. Semiconductors' properties are determined by the band gap between their valence and conduction bands.

In semiconductors with different valence and conduction bands, the photovoltaic effect occurs. While there are many other types of photovoltaic cells, this explanation will use a silicon based p-n junction since it is one of the simplest systems and because it dominates the commercial PV industry globally. Each atom is surrounded by and linked to its four neighbours in a silicon crystal lattice. The outermost electron shell of a silicon atom has four valence electrons. These four valence electrons are covalently connected with one of their closest neighbours, sharing one of the electrons. Covalent bonds, which connect two atoms together, are formed by shared electron pairs in semiconductors. Since two independent atoms cannot form a bond, these bonds exist. When a vacancy is filled, an

electron moves into it to fill it. As a consequence, a material that conducts electricity has been created (O.K. Simya, 2018).

The physics of solar cells are primarily related to the periodic crystal structure of semiconductors and will determine their electrical properties. Due to the magnetic fields around the component nuclei and the tightly bound core electrons, electrons that are confined to moving in semiconductor materials resemble particles in three-dimensional boxes with complex internal structures. Therefore, crystalline silicon solar cells currently occupy more than 90% of the market share (Lucio Claudio Andreani, 2018). Silicon is very important of being the second most plentiful element in the earth's crust. Furthermore, neither the manufacture nor the use of this substance is harmful to the environment.

2.4 Thin film

A thin film is made of a thin layer of material that are ranging in thickness from a few nanometers (nm) to a few micrometers (μm). There are two materials that used to produce thin films are silicon and ceramics. In many applications, a critical step enables the controlled synthesis of thin film materials in a process known as deposition. The most typical method for forming thin films is deposition, whether in physical or chemical. It's deposited on a substrate to obtain properties that are difficult to obtain in the bulk. The particular method a thin film is formed, in the form of successive addition of atoms or molecules, provides it its distinct properties. The important element of thin films is thickness, which is strongly linked with other properties that scale differently with thickness.

Thin film technology strikes at the core of solid state electronics' tremendous progress. The use of metal films' optical properties, as well as scientific curiosity in the behaviour of two-dimensional solids, have generated a rise in interest in thin film science and technology. Many new fields of research in physics and chemistry's solid state have been

advanced as a result of thin film research, which is based on characteristics that are specific to the thickness, geometry, and film's structure (West, 2003).

Thin film materials are critical components in optoelectronic, photonic, and magnetic device advancements. The ability to easily integrate materials into variety of devices is made possible by the formation of thin films from materials. When material characteristics are investigated as thin films, they differ significantly. Due to their particular properties such as electrical, optical, magnetic, or wear resistance, the majority of functional materials are used in thin film form. The technologies of thin film benefit from the fact that the thickness parameter has a significant impact on the properties. In this era of modern technology, both crystalline and amorphous thin films play an important role. Microelectronic devices, photoconductors, infrared detectors, solar cells, polarizers, superconducting films, anticorrosive and ornamental coatings are a few examples of the application created by thin film (Y. Gao & H. Niu, 2003).

Due to its effective solar energy conversion, solar energy has emerged as an alternative source to overcome the issue of energy shortage, as valuable earth natural resources such as fossil fuels and natural gas are nonrenewable and may be depleted over the next 10 years. Aside from that, using earth's natural resources may pollute the environment and affect the human health by emitting hazardous substances or gases during the burning of fossil fuels and natural gas. Thin-film solar cells have a variety of applications due to its easy to produce, low cost, and high-yield processing methods (Yadav and Masumdar, 2010). Therefore, suitable semiconductor materials are needed to produce thin-film solar panels that are both environmentally friendly and cost-effective with high conversion efficiency. Table 2.1 show the comparison of materials used in solar cells application.

Table 2.1 Comparison between materials that used in solar cells application

Solar cell type	Amorphous silicon (α -silicon)	Cadmium Telluride (CdTe)	Copper Indium Gallium Selenides (CIGS)
Achieved conversion efficiency (%)	8.3	14.6	21.7
Band gap (eV)	1.7	1.46	1.07
Advantages	<ul style="list-style-type: none"> • Low cost production • Mass production is simple. • Relatively high optical absorption coefficient • Excellent for small devices 	<ul style="list-style-type: none"> • Ideal band gap • High rate of light absorption • High conversion efficiency • Consistent result • Simple structure • Low cost production 	<ul style="list-style-type: none"> • Low cost production • Nonrecession • The substrate has a wide range of applications. • αh band gap is adjustable • Excellent antiradiation properties
Diadvantages	<ul style="list-style-type: none"> • Low conversion efficiency • Light-induced recession effect • Low stability 	<ul style="list-style-type: none"> • Limited natural tellurium reserves • Module and base material are expensive • Cadmium is toxic 	<ul style="list-style-type: none"> • Precisely control the difficulty of the four elements • Rare materials
Reference	Zhou <i>et al.</i> , 2014	Luo <i>et al.</i> , 2016	Salomé <i>et al.</i> , 2017

Thin film solar cells are valuable due to their low material consumption and improving efficiency. The three main thin film solar cell materials are amorphous silicon (α -Si), cadmium telluride (CdTe) and copper indium gallium selenide (CIGS). In order to compete with other photovoltaic technology, thin film silicon solar cells have an efficiency of up to 20%. The efficiencies of CdTe and CIGS are nearly similar to those of crystalline solar cells, which currently have a market share of more than 55%. The thin films of copper Indium Gallium Selenides (CIGS) able to produce 21.7%, which is the highest conversion efficiency (Salomé *et al.*, 2017). Due to its low efficiency and photodegradation, α -Si has almost extinct in terrestrial applications.

2.4.1 Thin Film Growth

Thin films are formed by depositing material atoms onto a substrate. Figure 2.2 represents the typical material atom deposition thin film growth process on a substrate. A random nucleation process are for thin film to form. It is used to start the nucleation and growth stages of all thin-film materials. The nucleation and growth phases are effected by several deposition conditions such as growth rate, growth temperature and substrate surface chemistry. The nucleation stage might be changed by external influences such as electron or ion bombardment. Film microstructure, film stress and associated defect structure are all influenced by the nuclear stage deposition situation. As a result, thin films' crystal phase and crystal orientation are determined.

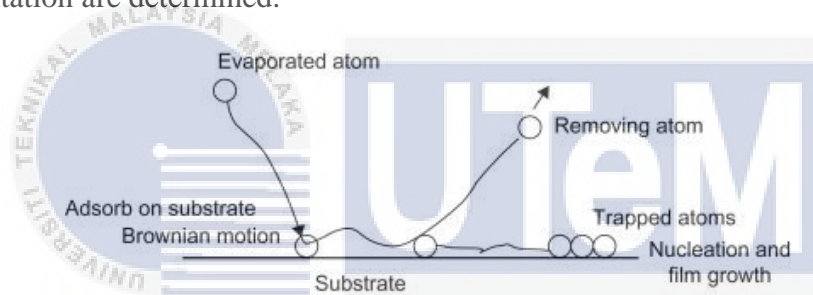


Figure 2.2 The growth models of thin film (Hideaki Adachi & Kiyotaka Wasa, 2012)

The process of solubility relaxation is another side effect of the thin film formation process. Films are doped and alloyed by allowing co-deposition during the atomic growth process. Since thin films are made up of individual atomic, molecular, or ionic species without any solubility limitations in the vapour phase, hence the solubility requirements between the various materials are rather flexible. This makes it possible to make multi-component materials like alloys and compounds with a larger compositions's range than bulk materials. As a result, materials with desired properties can be tailored, which giving materials technology a new and interesting dimension. This technique of tailor-made materials is represented by the production of hydrogenated amorphous Si films to be used in photovoltaic cells. By changing the optical band gap from 1 eV to around 2 eV and lowering

the dangling bond states's density in the band gap, hydrogenation allows doping of a (n and p) in amorphous silicon (Haris Mehmood & T. Tauqeer, 2017).

During the formation of thin films, films go through various phases, each of which has an impact on the microstructure of the film and hence its physical characteristics. The interaction between the energy on the substrate's surface and the surface energy on the thin film, as well as the energy of the thin film's interaction with the substrate, determines the thin film's growth mode. All systems aim to minimize their free energy by maximising the area of lowest energy surfaces while reducing interface energy wherever possible. The three involved interface energies, as well as maybe some strain, are the determining factors in the ensuing growth mode. Thin film nucleation and growth are influenced by the deposit's thermodynamic parameters as well as the atom-substrate interaction.

2.4.2 Growth Modes of Thin Film

The thin film growth is follow by nucleation process. The classification of this growth of thin film are divide into three modes which are layer-by-layer growth (Frank-van der Merve, FM), island growth (Vollmer- Weber, VW), and layer-plus-island growth (Stransky-Krastanov, SK).

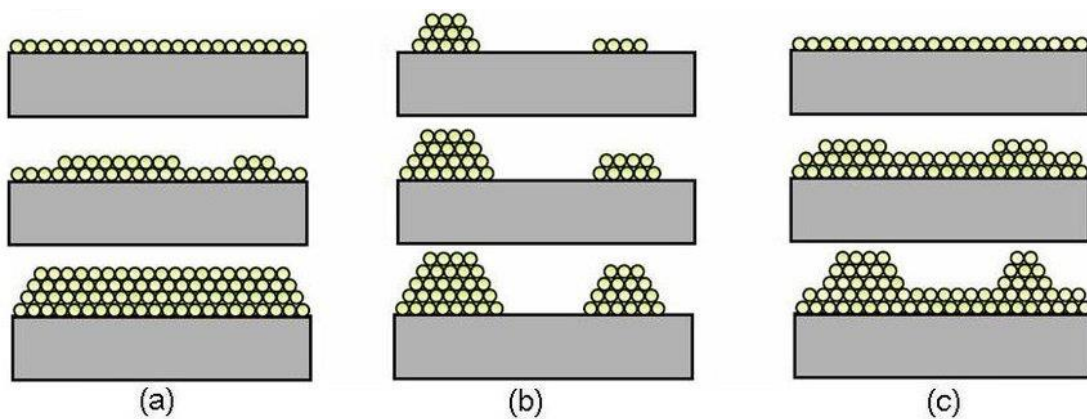


Figure 2.3 (a) Layer-by-layer growth mode (b) Island growth mode (c) Layer-plus-island growth mode (T. Devillers, 2008)

The film atoms are more closely attached to the substrate than to one other in the Frank-van der Merve (FM) layer-by-layer growth mode (Figure 2.3 (a)). First, a monolayer is produced, then the second layer is deposited. As a result, each layer is completed before the formation of next layer, resulting in exclusively two-dimensional growth. When the film and substrate are homogenous or distinct elements, such as semiconductor and oxide epitaxial growth, this growth mode occurs.

The island mode, also known as Vollmer-Weber (VW) (Figure 2.3 (b) mode, describes the situation in which film atoms are more tightly linked to one another than to the substrate. Three-dimensional islands emerge and grow immediately on the substrate surface in this situation. The 'islands' continual growth has resulted in a rough surface of polycrystalline thin films. When the substrate and the film are both heterogeneous, this happens..

Stransky-Krastanov (SK) (Figure 2.3 (c) shows the layer-plus-island mode which is mixing of the layer-by-layer growth and island growth. Both two-dimensional layer and three-dimensional islands is observed in this mode of growth. It happens when there is a stress impact as a result of two-dimensional development. The type and thickness of the intermediate layer are highly dependent on the substrate and chemical and physical characteristics of film, such as lattice parameters and surface energies , depending on the specific situation (for example, a surface phase that is submonolayer thick or a strained film that is many monolayers thick).

2.5 Cyclic Voltammetry (CV)

The electrodeposition method of thin film of semiconductor on ITO substrates can be investigated using cyclic voltammetry technique. Cyclic voltammetry plays an important role of tool in the study of electrochemistry since it investigates the electrochemical

behaviour of a system. It's one of the most important analytical properties for determining the current an electrochemical cell produces. The increased voltage is shown in the equation provided by Nernst. By cycling the voltage and measuring the resulting current, the working electrode performs this task. This electron transfer investigation can learn from this characterization study. The power of cyclic voltammetry is used to get the necessary information about the thermodynamic process of redox and the mechanism of electron-transfer actions. The most important factors for standardising photovoltaic systems include the prominent transfer of charge from donor to acceptor, charge transport, and charge collecting at the electrodes. The operational mechanism scans the electric potential before approaching the final potential, then reverses direction and scans the initial potential again. It's used to investigate redox processes and determine reaction product stability (Kumar *et al.*, 2016).

During the film deposition, cyclic voltammetry is an useful electro-analytical method to determine electrode potential. The potential of the working electrode is continually changed throughout time while the current produced by redox events is measured in this potential sweep technique (Nasirpour, 2016). Nowadays, cyclic voltammetry is the most commonly used electrochemical technique by researchers since it is an elegant method for analysing redox reactions at electrode solution interfaces that can be carried out with relatively simple equipment. A basic cyclic voltammetry experiment consists of a cell with three electrodes: a reference electrode, a working electrode (where the reduction or oxidation reaction occurs), and a counter electrode. This is a three-electrode setup. The species of interest is dissolved in the solution combined with an electrolyte that promotes conductivity. The solution is then injected with three electrodes. The working electrode has a small disc of electrode exposed, allowing the reaction to occur in a controlled environment. The circuit is completed with a counter electrode consisting of gold, platinum wire, or graphite. A

reference electrode with a known potential is an important element in cyclic voltammetry for measuring the potential supplied to the cell. Standard hydrogen electrodes, saturated calomel electrodes, and silver-silver chloride electrodes are all examples of reference electrodes (Aryan *et al.*, 2014). According to researchers, cyclic voltammetry provides extra information that may be used to draw conclusions about the reduction or oxidation reaction, as well as the stability of the species formed by electron transfer.

The current is recorded by sweeping the potential back and forth between the set boundaries (from positive to negative and negative to positive). The data obtained from CV may be applied to analyze about the material's electrochemical behaviour. The redox peaks, which are the material's reduction and oxidation peaks, which are determined from graphical analysis of a cyclic voltammogram, and are used to identify the electrode's capacitive behaviour. As a result, the potential for oxidation and reduction of the material can be determined. Figure 2.4 show the example of cyclic voltammetry.

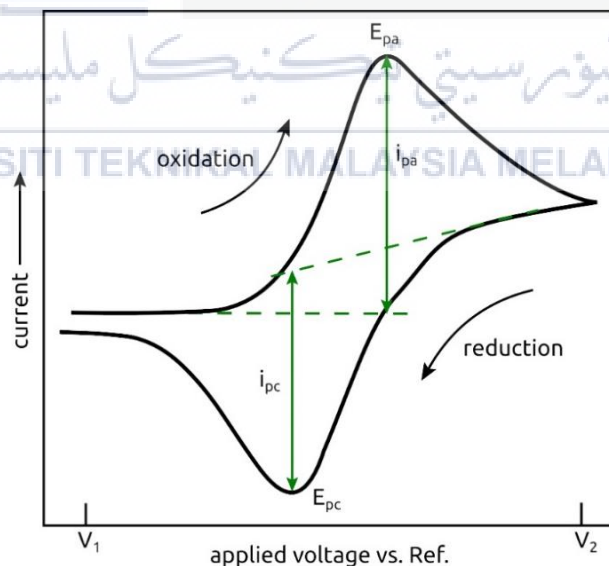


Figure 2.4 Cyclic voltammetry (Ying Zhuo, 2021)

2.6 Thin Film Deposition Method

A variety of substrate materials have been improved through thin film deposition in terms of optical, mechanical, chemical, tribological, and other properties (Diego Martínez-

Martínez, Herdes & Vega, 2017). The desired properties are determined by the resulting film structure, which is influenced by the deposition technique, substrate and film material. Due to the wide range of thin film applications, a number of deposition processes have been developed to optimise film characteristics. Physical vapour deposition (PVD) and chemical vapour deposition (CVD) are the two types of thin film deposition that are commonly used (Y. Deng & K. Tong, 2020). The physical characteristics of thin films are greatly influenced by the film preparation or thin film production procedure.

Physical vapour deposition (PVD) is a vaporisation coating process that includes atomic-level material transfer while chemical vapour deposition (CVD) is a chemical reaction process of depositing a crystalline lattice from a vapour that take place on or close a typically heated surface of the substrate that includes ion plating evaporation. The solid substance that results is either a thin film, powder, or a single crystal. When comparing physical and chemical deposition techniques, chemical deposition methods are preferable. Although physical deposition techniques can produce high-quality films, however scaling them up is difficult (Lai *et al.*, 2009).

Since the thin film of semiconductor has ion molecule, chemical vapour deposition (CVD) is suitable technique to produce thin film. It's made to produce thin films with controlled stoichiometry and morphology, whether they're single or multi-component (Canan Acar & Ibrahim Dincer, 2018). As a result, photocatalysis, dye-sensitized solar cells and photoelectrochemical cells generally use CVD to produce photoactive materials.

2.6.1 Electrodeposition

Electrodeposition, also known as electroplating, is an electrochemical process to deposit thin films by driving cations in the electrolyte to the cathode, which is usually a "inert" material (such as gold or platinum), where the cations are reduced to alloys, metals

or interact with one another to create a compound. In the electrodeposition setup, a reference electrode, the electrolyte, an anode, a cathode and a power supply that generates a constant DC current (galvanostatic) or a constant DC voltage (potentiostatic) are shown in Figure 2.5.

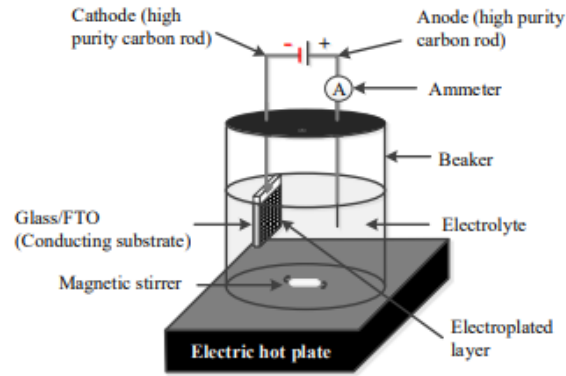


Figure 2.5 Electrodeposition setup (Ayotunde Adigun Ojo & Imyhamy Mudi Dharmadasa, 2018)

Since the procedure is normally carried out around room temperature, electrodeposition equipment is cheap, and the process is energy efficient. Materials utilisation in electrodeposition techniques can reach 100% if stable electrolytes with high lifetime are applied. In the situation of zinc coatings produced by roll-to-roll methods, ED is already a widely used technique in industry for mass production of large-section metallic coating materials (deposition rates in the tens of microns per hour, several metres per minute, several metre large plates, etc.). The use of this method is well-suited to the large-area photovoltaic industry, and it can benefit in the mass production of CIGS solar modules (Lincot *et al.*, 2004).

Electrodeposition is a widely used deposition method. Submerging the substrate and a counter electrode in the solution and applying a potential difference between them to generate an ionic species reaction on the substrate surface to allow deposition on the conductive surface. Electrodeposition as a thin film coating method can be used for the protection and decoration, as well as to improve the material's specific surface qualities.

2.6.2 Chemical Vapour Deposition (CVD)

The chemical vapour deposition is a versatile and fast process to promote film formation, leading to the formation of pure coatings with controlled porosity and uniform thickness, even on complicated or curved surfaces. Chemical vapour deposition procedures may be described as any process that involves the surface-mediated reaction of adsorbed precursors from the gas phase to produce a thin solid layer on a substrate. "Surface-mediated" refers to the fact that the solid film is created as a result of a heterogeneous reaction at the substrate surface. Thin films are deposited by CVD when vapour phase precursors react chemically with a solid surface. Figure 2.6 show a process of CVD.

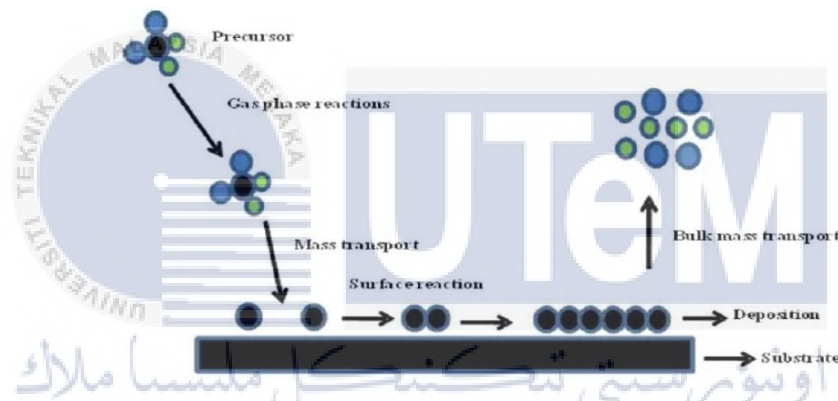


Figure 2.6 Aspects of a CVD process (Akhtar, M., 2013)

Chemical vapour deposition can be broken down into several stages: In order to use the CVD reactor, the precursor chemicals must be fed in first. Precursor molecules must be brought to the substrate surface once inside the reactor, generally through a mix of fluid transport and diffusion. The precursor molecule must stay on the surface for long enough for the reaction to take place once contact with the surface. The product thin layer atom must stay on the surface after the reaction, while the by-product molecules must desorb from the substrate surface to create space for further incoming precursor molecules.

CVD is a vacuum deposition method in which a volatile component of a deposition material reacts chemically between other gases to generate a non-volatile solid which is then

deposited on a substrate. This procedure can be used as a pre-coating like a pre-coating to improve substrate durability, reduce friction, and improve thermal properties—this implies that several deposition methods, such as PVD and CVD layers, can be used in the same coating (Damm, D.D., 2017). Unlike PVD, this technique does not require the reaction to be produced under vacuum. This technique allows the deposition of a variety of structures, including metal alloys and compound semiconductors, with high purity and doping (stoichiometric film) control, due to its versatility in working with a wide range of reactants and precursors (K. L. Choy, 2003).

2.7 X-Ray Diffraction (XRD)

XRD is an useful tool for analysing materials qualitatively and quantitatively, and it is most commonly used to identify unknown crystalline minerals. When X-Rays contact a crystal, they produce a series of unique and characteristic reflections for each phase, rather like a fingerprint (David Tavakoli, 2020). It is one of the most important techniques in crystallography and is widely used for structure determination in solid state physics. The geometry or structure of a molecule can be determined using X-rays. The XRD pattern obtained helps in the identification of different crystalline phases as well as the detailed analysis of their internal structural characteristics (Nutan S. Satpute & S.J. Dhoble, 2021). XRD methods are based on the X-ray's elastic scattering from materials having long range order. X-ray diffraction (XRD) is a method for identifying and analyzing atom location, arrangement in every unit of cell, and atomic plane spacing (Pappas, N., 2006). Minerals, plastics, polymers, ceramics, semiconductors, metals, and solar cells can all be investigated with XRD, which is a non-destructive testing process (Guma, T.N., 2012). Figure 2.7 show X-rays diffraction technique.

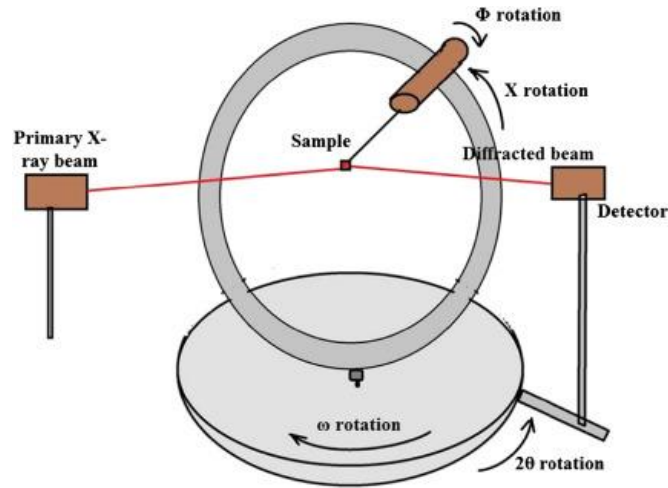


Figure 2.7 X-rays diffraction technique (Nutan S. Satpute & S.J. Dhoble, 2021)

Based on knowledge of basic XRD concepts as well as the structure of crystals in the materials needed, Hart, 1981 investigated alternative methods of Bragg's angle measurement. For the situation of $d > 10^{-4}$, single-crystal techniques were found to be common in various phrases. Fewster, 1999 evaluated many approaches for measuring lattice parameters. According to this study, the crystal structure's type has a great impact on the measurements methods that are acceptable.

Powder technique with diffractometer is most commonly used for thin films. The counter tube, which moves along the angular range of reflections, detects diffracted radiation in this method. A computer system keeps track of the intensities. To identify the unknown substance, the data of X-ray diffraction is tabulated on paper then compared to JCPDS data. Powder, single crystals, or thin films may be used as samples. Scherrer's formula, which is as follows, is used to calculate the size of crystallite of the deposits:

$$D_{XRD} = \frac{0.94\lambda}{\beta \cos\theta} \quad (2.1)$$

From Equation 2.1, D_{XRD} is the crystalline size (nm), λ is X-ray wavelength (nm) used ($\lambda=1.5418$), β is the diffraction line widening measured at half from its maximum intensity and θ is diffraction angle (Tlemçani *et al.*, 2015).

When electrons orbiting all around nucleus of an atom get to contact with solid objects, they scatter X-rays. These scattered waves interfere with each other since they are released in multiple directions. Depending on the type of wave interaction and direction, interference can be positive or negative. Diffraction is the constructive interference of dispersed X-rays. It's important to note that constructive interference is caused by the atomic structures of systematic arrangement in solids. As a result, it is evident how to evaluate crystalline substance of XRD graphs. Periodicity and diffraction have a close connection, with greater angle of diffraction associated with less periodicity and vice versa (Fultz, B, 2013). Figure 2.8 (a) and (b) show amorphous and crystalline materials in XRD graphs, respectively, from Lamas, D.G., 2017. Because amorphous materials lack a periodic arrangement, the XRD graph just shows the maximum average peak at a given in angle of diffraction, whereas crystalline materials have various peaks of XRD due to the atoms' periodic arrangement. XRD is also used to estimate the effects of treatment on the material crystallinity. For instant, a previous research (Sjöström, J.K, 2019) used XRD to investigate the effects of crystallinity on their tested samples with different treatments.

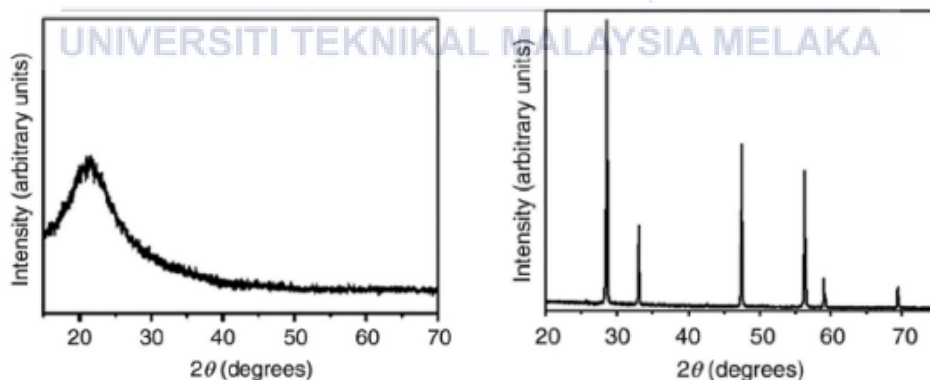


Figure 2.8 (a) XRD pattern of an amorphous material and (b) crystalline material (Lamas, D.G., 2017)

2.8 Scanning Electron Microscope (SEM)

Scanning electron microscope (SEM) are a useful tool for analyzing and photographing a variety of properties of materials, including structure, topography, light

emission and composition (J. Goldstein, 2007). SEM are commonly used to image topography by rastering the secondary electrons' intensity over a material's surface as a focused electron beam with an energy ranging from 100 eV to 30 keV. Components of Scanning Electron Microscope (SEM) are shown in Figure 2.9.

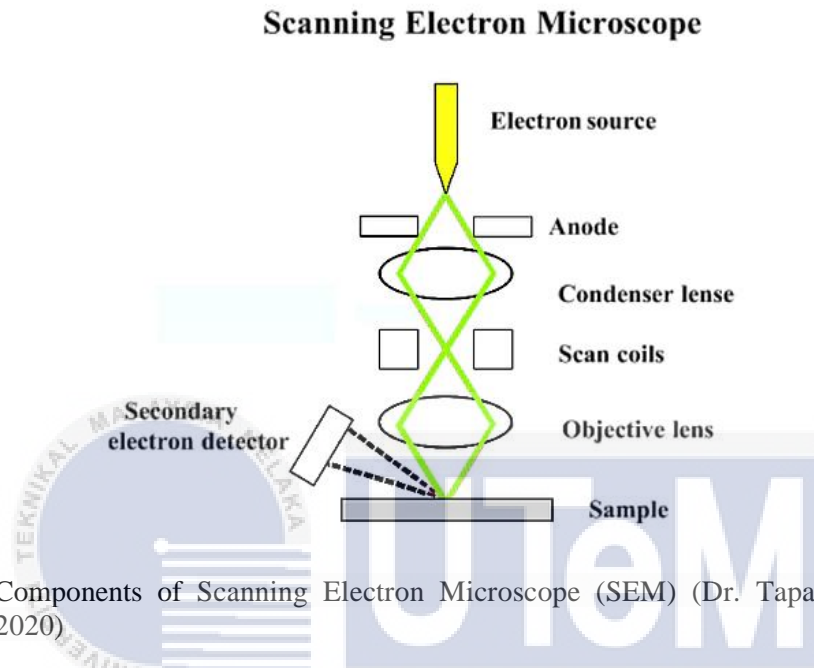


Figure 2.9 Components of Scanning Electron Microscope (SEM) (Dr. Tapanendu Kamilya, 2020)

In scanning electron microscope (SEM), microstructure morphology and chemical composition characterizations are examined and analysed by using a high-energy electron beam which is focussed. An electron beam on sample surface is interacted with using this technique. Due to elastic, inelastic, or photon scattering, this interaction creates the emission of electrons with varying energies from the sample, which are collected by a detector to produce a distribution map based on the signal intensities. The beam of electron is deflected in a magnetic field and moves in a raster pattern so that can capture the samples's surface. SEM scans a material's surface with a low-energy electron beam (generally between 1keV and 30 keV) with low nanometre-level resolution to produce images. Electron-sample interactions provide signals that show the crystalline structure, external morphology of sample (texture), chemical content and orientation of the materials used to produce the sample (Stokes, Debbie J., 2008). Due to the contrast produced by the

secondary electrons, this technique allows viewing of the crystalline columns forming at the sample surface, as well as the different material phases, either crystalline or amorphous, while a cross-sectional SEM study can be used to determine the film thickness.

Figure 2.10 shows deposition of CdTe films of SEM micrographs at temperatures which are from 500 °C to 700 °C. The grain size is proportional to temperature, as may be shown in SEM morphological images. The SEM images might show a huge grain formed by a group of small crystallites that is difficult to resolve to individual crystallites (Rahman Kazi Sajedur, *et al.*, 2019). Size of grain grown by an average of 20µm at high temperatures. As shown by the SEM results, the structure of bulk and average grain size is initially related to the deposition temperature with relation to the thickness.

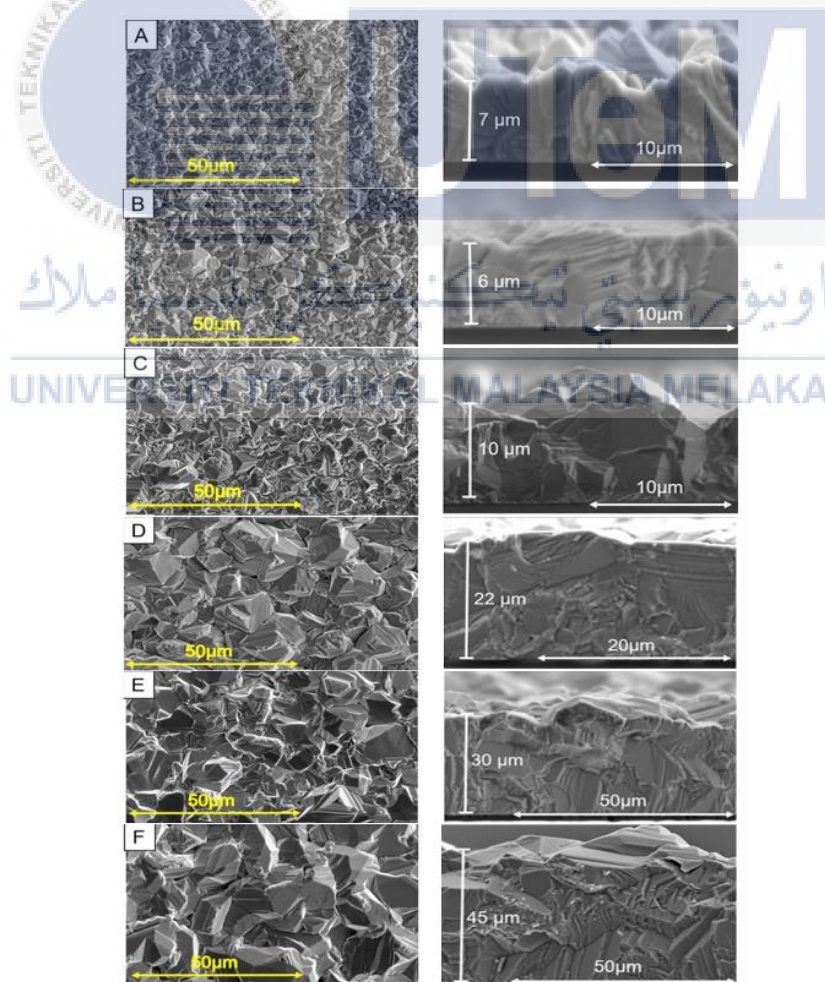


Figure 2.10 SEM images of CdTe thin films in surface morphology and cross-section view (Rahman Kazi Sajedur, 2019)

2.8.1 Scanning Electron Microscopy (SEM) Based Energy Dispersive X-ray Spectroscopy (EDX)

Energy Dispersive X-ray Spectroscopy (EDX) is a method that is used in combination with electron microscopy to determine elemental analysis and chemical composition. The procedure is produced as a result characteristic X-rays that show the identification of the components shown on the sample. This technique is commonly used with scanning electron microscopy (Karina Torres-Rivero, 2021). The EDX has been used in a number of sectors for compositional analysis. For example, the composition of the thin film deposited can be determined by EDX analysis. Erat *et. al* (2008) investigated CdSe thin films using the EDX method. Figure 2.10 shows the study results.

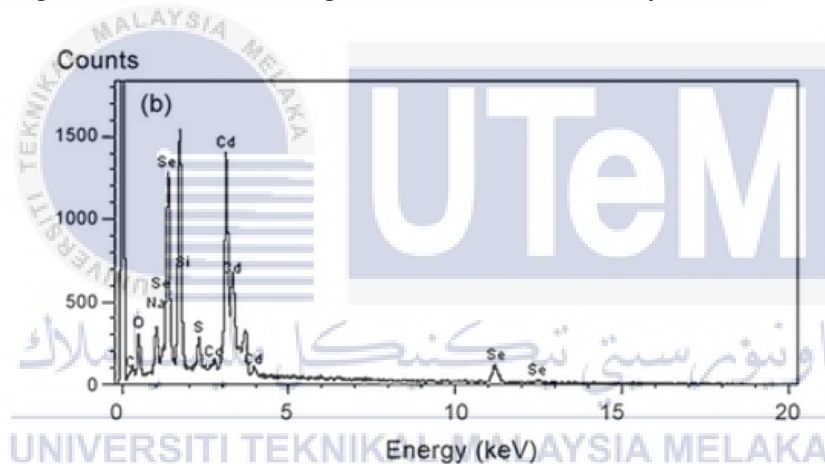


Figure 2.11 EDX result on CdSe thin film (Erat *et. al*, 2008)

Figure 2.11 shows the EDX result on a CdSe thin film. The presence of Cadmium and Selenium in the thin film composition can be seen from the results. The peak obtained from the EDX result is used to determine the composition.

2.9 Optical properties by Ultraviolet-Visible-Near Infrared (UV/Vis/NIR) Spectrophotometer

When a material is exposed with light, electrons are moved from lower to higher levels atomic or molecular orbitals, therefore spectroscopy in the ultraviolet (UV), visible

(Vis), and near-infrared (NIR) regions of the spectrum of electromagnetic is referred to as electronic spectroscopy (Weckhuysen, B. M., 2000). The band gap energy and optical properties of thin films were investigated using a UV/Vis/NIR spectrophotometer.

The absorption of light by a sample is the basis of UV/VIS spectrophotometer. Absorption by crystalline lattice, interband (fundamental) absorption, excitonic absorption, dopant absorption and absorption by free charge carriers are all examples of light absorption processes in semiconductors. When electrons are optically excited from the valence band to the conduction band, they create electron-hole pairs, which is known as fundamental absorption. Light absorption processes must correspond to energy and momentum conservation principles. If the energy of photons reaching a material more than the band gap energy, the emitted photon will move an electron from the valence band to the conduction band. The energy change of a quantized system can be described using the following formula:

$$\Delta E = h\nu = hc/\lambda = E_{ph} \quad (2.2)$$

where ν indicates electromagnetic radiation frequency, c represents the light speed in vacuum, and w means the vacuum wavelength of photon. Absorption spectroscopy are used to gain data on electronic transitions inside the d-orbitals of transition metal ions, defects, or band gap transitions in between valance and conduction bands in the UV-Vis range which are from 200nm to 350nm in this case (Förster, H., 2004). The Tauc Plot is a technique for determining the band gap using spectrophotometer results. According to the Tauc, Davis Mott relation,

$$(\alpha h\nu)^{1/n} = B(E_{ph} - E_g) \quad (2.3)$$

where h is Planck's constant, ν is frequency of vibration, α is coefficient of absorption, E_g is band gap, n is 1/2, 3/2, 2 or 3 depending on band gap type, B is constant of proportional and

n is the transition probability; it takes values as 0.5, 1.5, 2 and 3 for direct allowed, direct forbidden, indirect allowed and indirect forbidden, respectively.

Direct band gap semiconductors and indirect band gap semiconductors are the two types of semiconductors. The top of valence band and bottom of conduction band in figure 2.12 (a) overlap in the k -space position (wave vector's space), however they do not overlap in figure 2.12 (b). In direct-gap semiconductors, the electron move from valence band to conduction band towards the fundamental absorption's edge requires only photon absorption. In indirect semiconductor, however, the presence of an extra particle that may affect the electron's momentum is necessary. A phonon (quantum vibrations of crystal lattice) is an example of this type of particle. It is commonly known that as the number of particles involved in the process increases, the probability of the process decreases. As a result, indirect semiconductors have low intensity light absorption at the absorption edge than direct-gap semiconductors. This fact is very important in the field of photovoltaic devices. Solar cells made of indirect band gap semiconductors (such as silicon) require thick (a few hundred micrometres) layers to absorb the heat effectively (Roy, P. & Srivastava, S. K., 2006). As a result, as material consumption increases, the requirements for material quality (recombination losses will be considerable if optical carriers are produced out from the p - n junction in a highly imperfect semiconductor). However, in direct band gap semiconductors (such as CIGSS or CdTe), absorber layers as thin as a few micrometres are sufficient, and material quality can be relatively poor. As a result, solar cells made of thin films with a direct band gap materials attain the lowest cost produced photovoltaic energy (N. R. Paudel & Y. Yan, 2014).

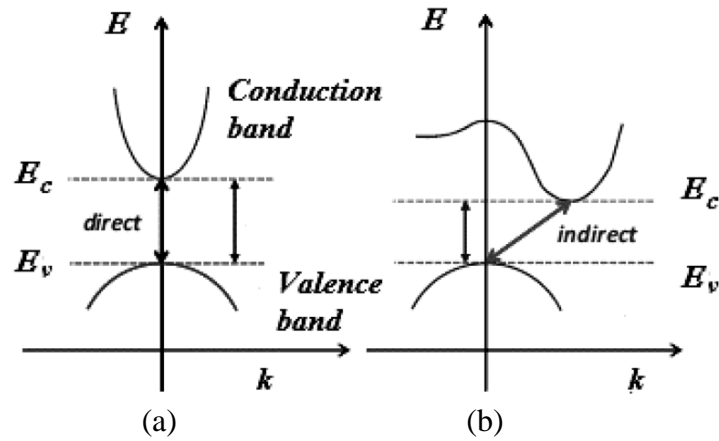


Figure 2.12 Band diagram of semiconductor for (a) direct band gap and (b) indirect band gap (Amelia Carolina Sparavigna, 2014)

Tin oxide (SnO_2) films are ideal for solar cell applications according to Rameshkumar and co-workers (B. Rameshkumar, A. Anderson, D. Ananth & T. Mohan, 2021). These materials will absorb the most UV light before dropping into the visible range. The maximal optical transmittance was at 70-80%, with a 287 nm cut-off frequency. Another study of the optical absorption of CdTe/CdS thin films was carried out using a UV-Visible spectrophotometer has shown a wavelength range of 300-1100 nm. Figure 2.13 shows the optical band gap of CdTe and CdS thin films, which was determined from the graph $(\alpha h\nu)^2$ versus photon energy ($h\nu$). The intercepts of a straight-line that extrapolated zero absorption coefficients on the axis of photon energy. The band gaps meet the reported values very well (F.Lisco, 2015). CdS has a 2.4 eV band gap, while CdTe has a 1.36 eV band gap. The values of band gap of CdTe and CdS thin films were calculated using Equation 2.3.

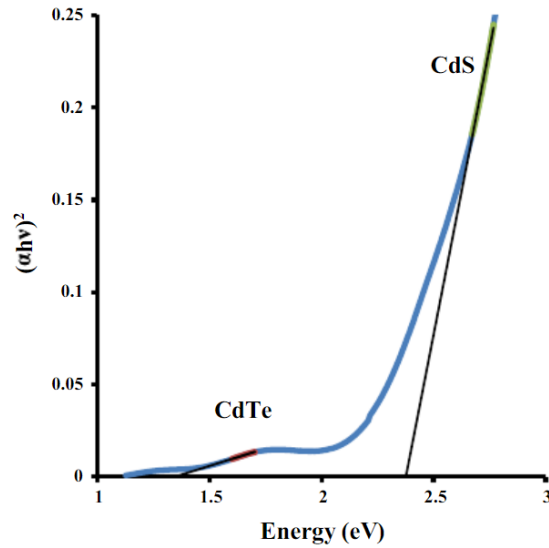


Figure 2.13 $(\alpha hv)^2$ plots with respect of photon energy (hv) for CdTe/CdS thin film (K. N. Nithyayini & Sheela K. Ramasesha, 2015)

2.10 Photoelectrochemical Studies

The semiconductor parameter can be used to determine the photoelectrochemical solar cells factor of a semiconductor compound. Semiconducting properties like as doping density, band bending, valence band edge, and others can be calculated using the Mott Schottky plot. The inverse of square of capacitive versus the applied potential to thin films is plotted to tabulate potential-capacitive behaviour data (Anand & Shariza, 2012). In Mott-Schottky graphs of $1/C_{SC}^2$ against V_{SCE} , the interception of give that flat band potential V_{fb} .

The Mott-Schottky equation is as follows in experimental voltages:

$$1/C_{SC}^2 = \frac{2(V - V_{fb} - (kT/q))}{\epsilon_S \epsilon_0 q N_D} \quad (2.4)$$

where C is the space charge capacitance, V_{fb} is the flat band potential, ϵ_S is the semiconductor dielectric constant, ϵ_0 is the free space permittivity (8.854×10^{-12} F/m), q is the electronic charge (1.603×10^{-19} C), N_D is the doping density, k is the Boltzmann's constant (1.38×10^{-23} J/K) and T is the temperature of the operation. The slope of straight line can also be used to calculate N_D .

The dielectric constant, ϵ for the thin films can be calculated by using:

$$\epsilon = Cd/A\epsilon_0 \quad (2.5)$$

where the C represents for capacitance, d is the thickness for crystal and A for area of contact.

The width of the depletion layer (W) and the band bending (V_b) are two important key parameters to determine:

$$V_b = V_{F,redox} - V_{fb} \quad (2.6)$$

$$W_{1/2} = (2\epsilon\epsilon_0 V_b/eN) \quad (2.7)$$

where V_b is the built in voltage or the band bending and $V_{F,redox}$ is the redox potential of the $2I^-/I_2$ redox couple, which is equal to $0.295 V_{SCE}$ (Lokhande *et al.*, 2002). N_C is the density of states, N_C that can be written as:

$$N_C = 2/h^3 (2\pi m_e * kT)^{3/2} \quad (2.8)$$

where h is the Plank's constant (4.136×10^{-15} eVs), m_e is the effective electron mass in the conduction band. The measurement of capacitive as a function of applied voltage (i.e. Mott-Schottky plot) gives useful data such as the type of conductivity, depletion layer width and flat band potential (V_{fb}), which could provide an understanding about the critical semiconductor properties of thin films for use as photoelectrochemical cell elements.

The semiconductor's flat band potential, V_{fb} is a key factor to understand movement of the electrons across the semiconductor-electrolyte junction. Since band bending provides the highest feasible output photovoltage from a semiconductor-based device, selecting redox systems with $V_{F,redox}$ near to E_v for n-type semiconductor photoanode solar cells would be preferable from an efficiency stand point. In general, the efficiency of a material's conversion depends greatly on its properties. The maximal efficiency under light excitation is given by (Gujarathi *et al.*, 2006):

$$\eta_{max} = eV_b / E_g \quad (2.9)$$

where V_b is band bending and E_g refers to the energy gap (obtainable via Mott-Schottky plots and optical properties). The maximum efficiency is defined by band bending and the energy gap, as shown in the formula above. As a result, in a photoelectrochemical cell, the higher the value of band bending, the higher the photoconversion efficiency. As a result, higher photoconversion efficiency is related to increased thickness of the film, which is the result of

- (i) reduction in the band gap (E_g);
- (ii) increase in the band bending, V_b of the material in longer-deposited films (i.e. higher thickness).

The Mott-Schottky plot for of NiSSe thin films is a good example. S.Shariza and Anand (2018) investigated the thin film of NiSSe by plotting the Mott-Schottky is shown in Figure 2.14 and its corresponding flat band potential of the thin film of NiSSe from the Mott-Schottky plots in Table 2.3. The flat band potential value of the junction is determined by the intersections of plots on the voltage axis. The Mott-Schottky plot for NiSSe thin films at different deposition times is shown in Figure 2.14. It shows a Mott-Schottky plot with negative slopes, highlighting that the deposition of films have p-type conductivity. In solar cell applications, the value of V_{fb} is important since it defines the maximum allowable cell photovoltage.

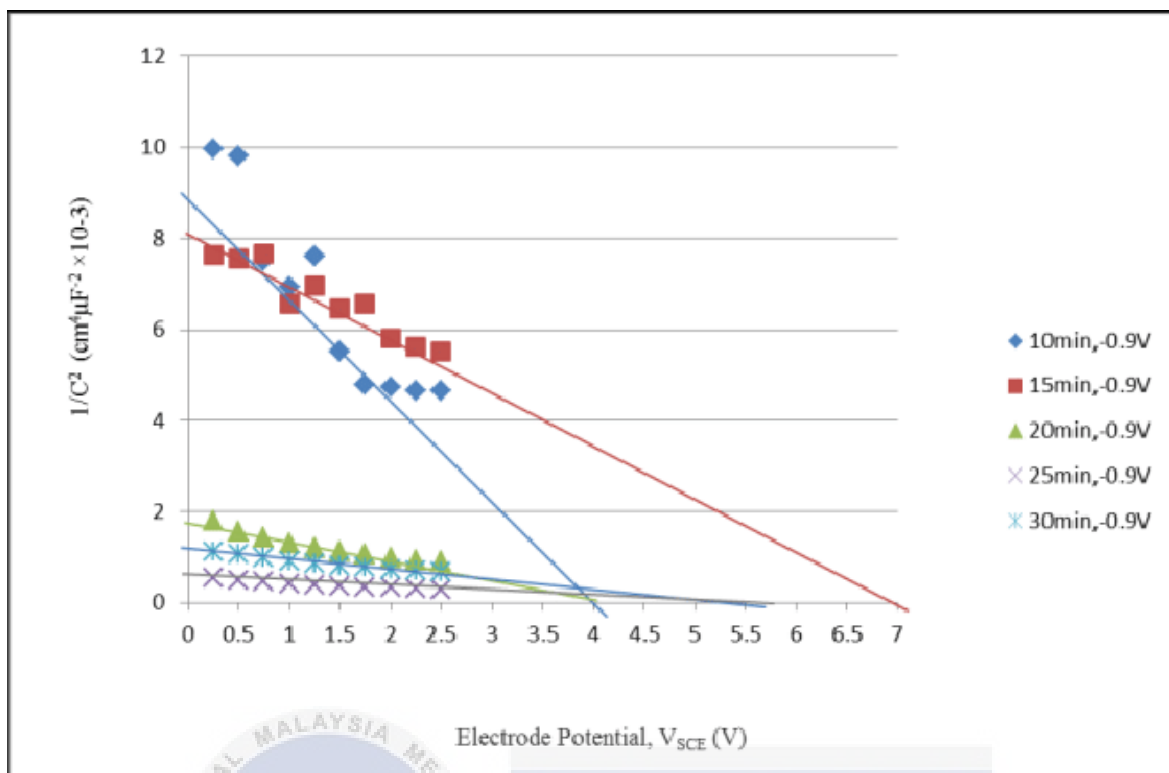


Figure 2.14 Mott-Schottky plot of NiSSe thin film (S.Shariza & Anand, 2018)

Table 2.2 Flat band potential for thin films of NiSSe (S.Shariza & Anand, 2018)

As deposited sample with respect to deposition time	Flat band potential (V_{fb})
-0.9 V, 10 min	$4.0 \pm 0.02 V_{SCE}$
-0.9 V, 15 min	$7.0 \pm 0.02 V_{SCE}$
-0.9 V, 20 min	$4.5 \pm 0.02 V_{SCE}$
-0.9 V, 25 min	$5.0 \pm 0.02 V_{SCE}$
-0.9 V, 30 min	$3.75 \pm 0.02 V_{SCE}$

As shown in Figure 2.15 below, the positive slope confirms the n-type conductivity of the NiS₂ film. The semiconductor electrode potential at which band bending is zero is determined as the intercept of the linear plot ($1/2 C_{SC} = 0$). This potential is equivalent to 0.48 V_{SCE} and is called the flat-band potential.

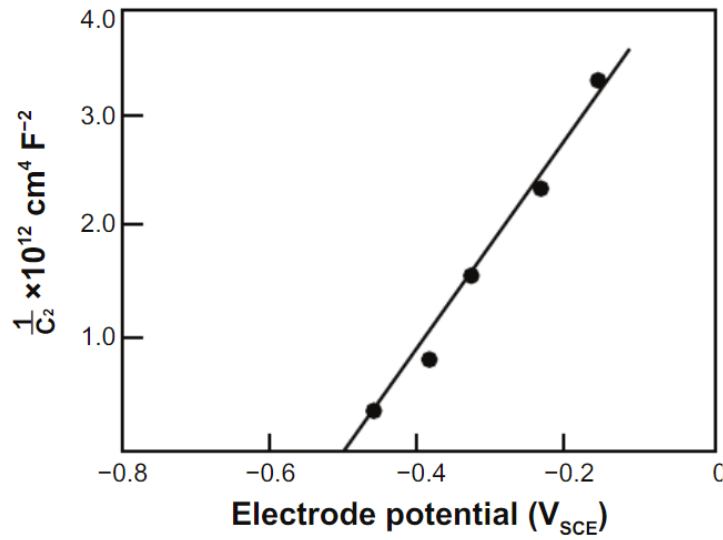


Figure 2.15 Mott-Schottky plot of NiS₂ thin film (Anand, 2013)

2.11 Summary or Research gap

The literature review informs us about provides proper photoclectochemical cell materials and their semiconducting characteristics, as well as the properties of Molybdenum diselenide (MoSe₂) thin films. Existing materials including Silicon, Molybdenum dilsulfide (MoS₂), Cadmium Telluride (CdTe) and Copper Indium Gallium Selenides (CIGS) have been used in the PEC, but the efficiency is only around 13-14%. It was also found that existing materials are very costly. Electrodeposition, a CVD process, was chosen as a synthesis method because of its high deposition scale, low cost, and efficient control of layer thickness of thin film. The band gap range of good semiconducting materials is 1-3 eV in nature.

As a result, in response to the above-mentioned problem, there is a research way to discover, study and build new, efficient and integrated techniques and methodology for the Molybdenum diselenide (MoSe₂) thin films used in photoelectrochemical solar cells. Therefore, there are some summaries that can conclude from this research gap are:

- i. Molybdenum diselenide (MoSe_2) thin films can prepared by using cyclic voltammogram reduction potential.
- ii. Optical analysis of Molybdenum diselenide (MoSe_2) thin films can studied by using a UV/Vis/NIR spectrophotometer.
- iii. Semiconductor parameters can determined from a Mott-Schottky plot.

The goal of thin film is to achieve efficiency and high accuracy. This thesis is mostly concerned with this topic. The following Chapter 3 would cover the experimental technique used in this research.



CHAPTER 3

METHODOLOGY

3.1 Introduction

The experimental technique performed in this research for the synthesis and optical of Molybdenum diselenide (MoSe_2) thin films was discussed in this chapter. Physical and chemical vapour deposition techniques are the two basic types of thin film deposition. Sputtering, molecular beam epitaxy (MBE), sulphurization, spray pyrolysis, chemical bath deposition and electrodeposition are among the most often used processes. Due to its intrinsic benefits, such as high deposition rate, accurate control over film thickness and morphology, mass production, and low manufacturing costs, the electrodeposition process has recently attracted great attention (Yang *et al.*, 2015).

For electrodeposition, potentiostat and galvanostat modes are available. Potentiostats are electronic devices that control the voltage differential between the reference and working electrodes, whereas galvanostats are used to control the device's ability to maintain the current flowing through the process. In order to synthesis MoSe_2 thin films in a potentiostatic mode, an electrodeposition technique would be used. Then, the thin film's structure and its morphologies are investigated using X-ray diffraction (XRD) and Scanning Electron Microscope (SEM). Energy Dispersive Spectroscopy (EDX) used to determine the compositional analysis that would give their stoichiometric relationships. UV/Vis/NIR Spectrophotometer and Mott-Schottky plot are used to determine the optical studies of the of MoSe_2 thin films. Figure 3.1 shows the flow chart for the experimental procedure for the research.

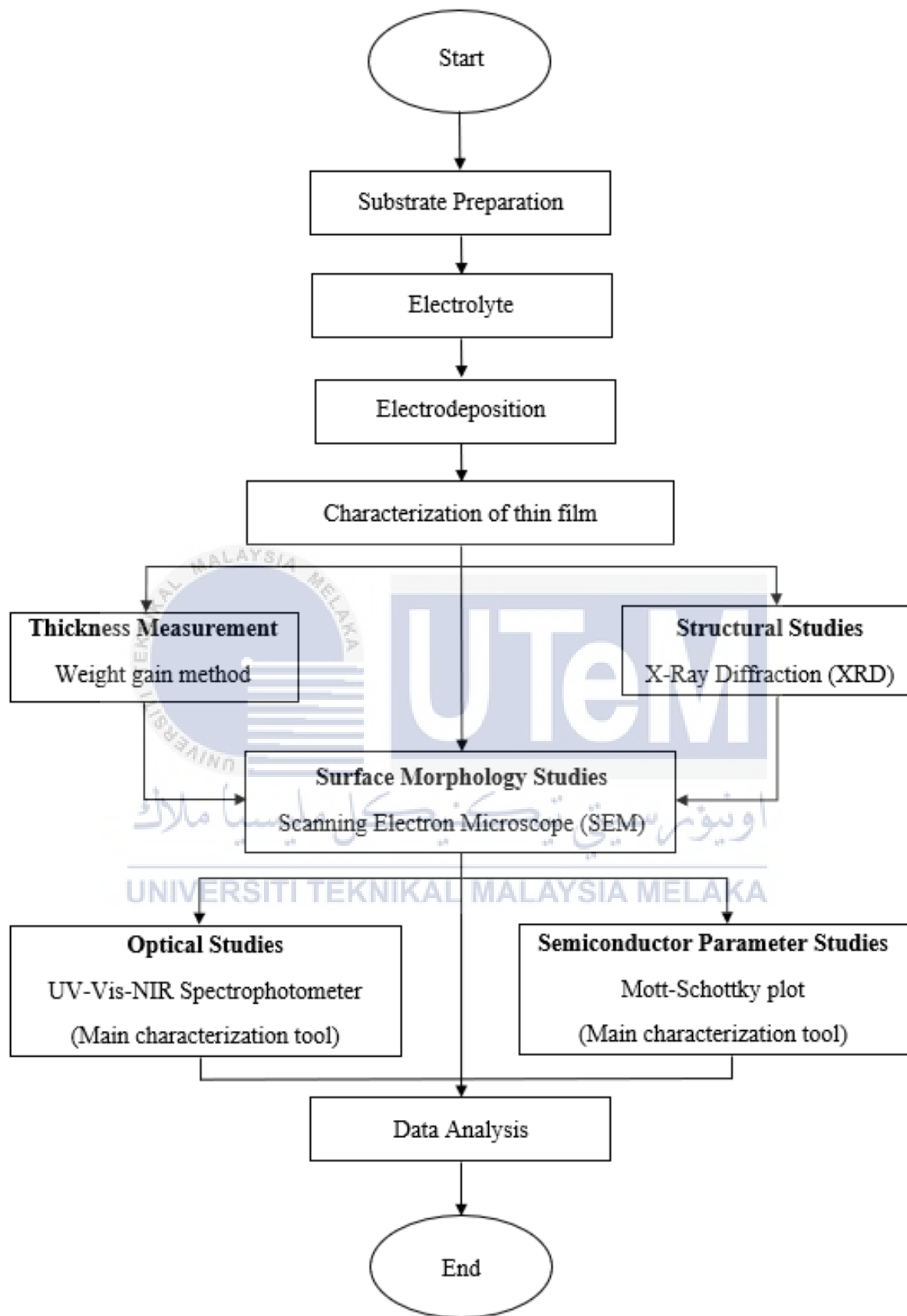


Figure 3.1 Flow chart of this project

3.2 Substrate Preparation

In this project, the substrates for depositing MoSe₂ thin films would be indium tin oxide (ITO) coated glass. For the thin film deposition, the ITO coated glass substrate would be cut into 2.50 cm × 1.50 cm × 0.20 cm size using a diamond cutter. The substrates would be dipped in 50% dilute hydrochloric acid (HCl) (Sheet, 2013) for 15 minutes, rinses with double distilled water and then clean with hot air before film deposition. This type of treatment improves electrodeposit adhesion to surfaces, allowing for thicker deposition without peeling. As a result, the substrates are prepared for cyclic voltammetry (CV) and electrodeposition.

3.3 Synthesis of MoSe₂ thin film

The cyclic-voltammetry (CV) used to determine the deposition potential of MoSe₂ and the standard potential range of +2.0V to -2.0V and +1.0V to -1.0V was used for the analysis. The MoSe₂ were synthesized using electrodeposition method. The electrodeposition setup was using the three-electrode cell deposition method with counter electrode (anode) that made up using graphite or platinum, working electrode (cathode) that made up using an Indium Tin Oxide (ITO) coated glass substrate and reference electrode (RE) that made up by using Saturated Calomel Electrode (SCE). Mo⁴⁺ and Se²⁻ ion sources were employed as predecessors in this investigation. The ratio of each material for Mo:Se is selected to be 1:2. Using the Princeton Applied Research Model VERSASTAT 3 Potentiostat, the cyclic voltammetry (CV) of range of potential value is changed to -1.20V to define the best potential value for electrodeposition to occur. After determining the appropriate deposition potential, the thin film deposition times were set to 10 minutes, 20 minutes, 25 minutes, and 30 minutes. The electrolyte solution is kept at a room temperature

in the bath. The cyclic voltammetry and electrodeposition experimental setup is shown in Figure 3.2.

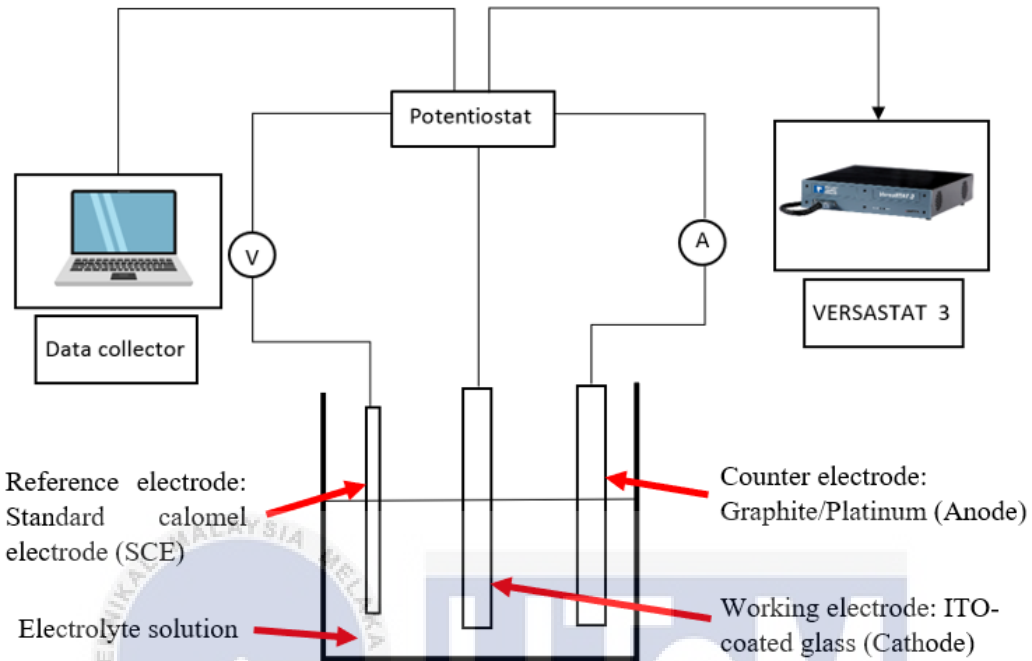


Figure 3.2 Electrolytic cell setup of MoSe₂ thin film deposition

3.4 Film Thickness Measurement

The gravimetric weight difference method was used to determine the thickness of film. In this method, the thin film sample must be thoroughly cleaned to remove all interfering contaminants. The ITO-coated glass substrates were carefully cleaned and dried before the electrodeposition. An analytical balance weighing equipment with four decimal points was used to weight the ITO-coated glass substrates. The weight of the ITO-coated glass substrate is obtained immediately after deposition to determine the weight gain due to the thin layer formed. The difference in weight before and after deposition was inserted into Equation 3.1 to determine the film thickness.

$$\text{Thickness (cm)} = \frac{\text{Mass (g)}}{\text{Density (g/cm}^3\text{)} \times \text{Area (cm}^2\text{)}} \quad (3.1)$$

3.5 Structural Studies by X-ray Diffraction (XRD)

The MoSe₂ thin films were analyzed using X-ray Diffraction (XRD) for its structural characterization. Molybdenum diselenide (MoSe₂) in the film can be confirmed using XRD. The thin film's X-ray diffractograms were obtained by using a PAN analytical XPERT PROMPD PW 3040/60 diffractometer (Figure 3.3) in order to calculate the lattice parameters to ensure that the results were supported by the report values and to analyse the crystallography of the thin films's stoichiometric. The structural information of the MoSe₂ thin film can be obtained with the use of monochromatic CuK α radiation ($\lambda = 1.54056 \text{ \AA}$) at 2θ angle in the range of 10° - 90° . The Joint Committee of Powder Diffraction Standards (JCPDS) document was used to index the XRD peaks that were identified. The spacing between the interplanar (d-values) were compared from X-ray diffractograms using the Joint Committee on Powder Diffraction Standards (JCPDS).

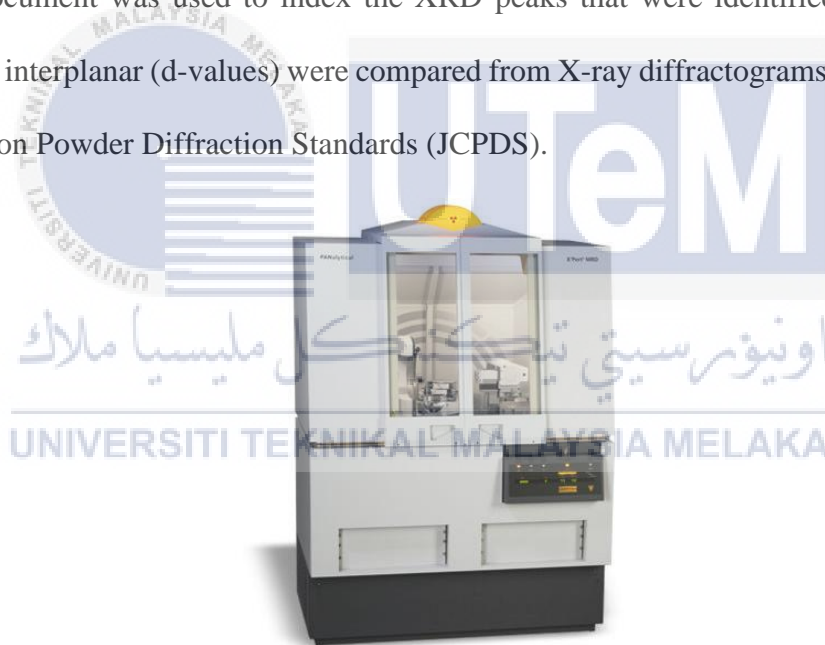


Figure 3.3 X-ray diffractometer XPERT PROMPD PW 3040/60 (Mohd Shahrulrizan Bin Ibrahim, 2021)

3.6 Surface Morphological Studies by Scanning Electron Microscope (SEM)

The MoSe₂ thin films were investigated by using SEM, JSM-6400 JEOL have been shown in the Figure 3.4 for its morphological properties. The SEM is a detector that converts X-ray radiation into voltage signals, which are then transmitted to a pulse detector to be measured. The signal would then be sent into an analyzer, which would display and evaluate

the data. The resulting micrograph is in planar view, and the surface structure was analysed to identify the shape forming on the substrate surface. The microstructural surfaces of the thin films were observed using SEM analysis. The state of the grain would be shown, and it would be determined whether the pin-hole-free morphology would improve grain contact. Energy Dispersive X-ray Spectroscopy (EDX) based on SEM had also applied in the research to study the thin film's composition. The stoichiometry of the MoSe₂ thin film was determined using SEM based EDX.



Figure 3.4 JSM-6400 JEOL Scanning Electron Microscope (SEM) (ebay, 2022)

3.7 Optical Studies by UV/Vis/NIR Spectrophotometer

A UV/Vis/NIR Spectrophotometer was used to analyse the optical absorption spectrum of MoSe₂ thin films with wavelengths ranging from 200 nm to 1100 nm in order to investigate their optical properties. A spectrophotometer is shown in Figure 3.5. The optical band gap of thin film is calculated from transmittance and reflectance according to Equation 3.2 by using the graph plot of $(\alpha h\nu)^n$ versus photo energy ($h\nu$).

$$E = h\nu = \frac{hc}{\lambda} \quad (3.1)$$

where h is the Plank's constant (6.63×10^{-34} J/S), ν refers to the frequency, λ refers to the wavelength and c is speed of light (3×10^8 m/s).

The optical band gaps of these compounds are determined by the intercepts on the energy axis at $\alpha=0$. Optical absorption measurements at the fundamental edge are predicted from the films, which is then used to analyse the band gap of the MoSe₂ thin film.



Figure 3.5 UV-Vis-NIR Spectrophotometer (EVISA, 2003)

3.8 Semiconductor Parameter by Mott-Schottky Plot

A potential-capacitance data of MoSe₂ thin film would be tabulated to establish its suitability for use as a solar cell material. The graphing of the power of negative 0.5 of space charge capacitance versus the applied potential V_{SCE} to the thin film is known as Mott-Schottky plots. Using an LCR Bridge meter, the capacitance value reflected by the voltage applied to MoSe₂ would be measured. The flat band potentials on the graph of $1/C_{SC}^2$ versus V_{SCE} was shown the flat band potentials, V_{fb} of the junction, according to the intercept of Mott-Schottky plot on the applied voltage axis.

Other semiconducting parameters, such as semiconductor type (n-type or p-type), width of the depletion layer (W), band bending (V_b), conduction band density of states (N_c), energy gap (E_g) and Fermi level of the semiconductor below conduction band can be determined using the Equation 3.3.

$$1/C_{SC}^2 = \frac{2(V - V_{fb} - (kT/q))}{\epsilon_s \epsilon_0 q N_D} \quad (3.3)$$

where C is the capacitance of space charge, k is the Boltzmann's constant (1.38×10^{-23} J/K), ϵ_s is the semiconductor dielectric constant, ϵ_0 is the free space permittivity (8.854×10^{-12} F/m), q is the electronic charge (1.603×10^{-19} C), T is the temperature of the operation and N_D is the doping density.



CHAPTER 4

RESULTS AND DISCUSSION

4.1 Introduction

This chapter describes the experimental results and the findings of this research. To achieve a better understanding, the information obtained through the procedures stated in the preceding chapter was identified and translated into graphical forms. The data analysis is used to create a brief description and discussion. This chapter includes some technical opinions and professional insights to enrich the collected results and help the discussion.

Molybdenum diselenide (MoSe_2) thin film synthesis used the electrodeposition technique. The technique was used with various deposition times. All of the samples were electrodeposited at a potential of -1.2V . These samples are then left in the open air to dry before going through the material characterisation procedures. Before and after the electrodeposition procedure, the mass of the ITO-coated glass substrate is measured on a micron scale to determine the thin film's thickness.

Other material characterization techniques include X-Ray Diffraction (XRD) analysis, Scanning Electron Microscope (SEM), UV-Vis-NIR spectrophotometer, Mott-Schottky measurement, and UV-Vis-NIR spectrophotometer. These techniques are used to analyse the structural and crystallinity of thin films, to study the surface morphology of all the samples, and to determine the optical properties. Through tables and graphs, data from various material characterization methods are analysed and understood. The initial goal of this study, which was to synthesise stoichiometric Molybdenum diselenide (MoSe_2) thin films using the electrodeposition method, was accomplished using the electrodeposition

process results. Additionally, interpretation of the results allows for validation of the optical characterization of Molybdenum diselenide (MoSe₂) thin films. After the results and discussion are finished, the Molybdenum diselenide (MoSe₂) thin film semiconductor parameters are determined.

4.2 Film Thickness Measurement

The mass of the ITO coated glass substrate before and after the deposition process is measured using a micron scale weight machine. The mass of deposited thin film on the substrate is defined as the difference between the two masses. The density for Molybdenum Chalcogenide (MoSe₂) film is 6.90 g/cm³ (Haynes, W. M, et. al., 2011) and the dimension of the substrate is 2.50 cm × 1.50 cm × 0.20 cm. The formula below determines the space area of ITO coated glass used to deposit.

$$\begin{aligned} \text{Surface Area} &= \text{Length} \times \text{Width} \\ &= 2.50 \text{ cm} \times 1.50 \text{ cm} \\ &= 3.75 \text{ cm}^2 \end{aligned}$$

The thickness of thin films is estimated using Equation 3.1, which is discussed in Chapter 3. The result is determined as given in Table 4.1 below.

Table 4.1 Thickness of MoSe₂ thin films

Deposition Time (minutes)	Mass of thin films (g)			Film thickness (µm)
	Before Deposition	After Deposition	Difference	
10 minutes	0.5344	0.5462	0.0118	4.560
20 minutes	0.6116	0.6363	0.0247	9.546
25 minutes	0.5420	0.5166	0.0254	9.816
30 minutes	0.5631	0.5891	0.0260	10.048

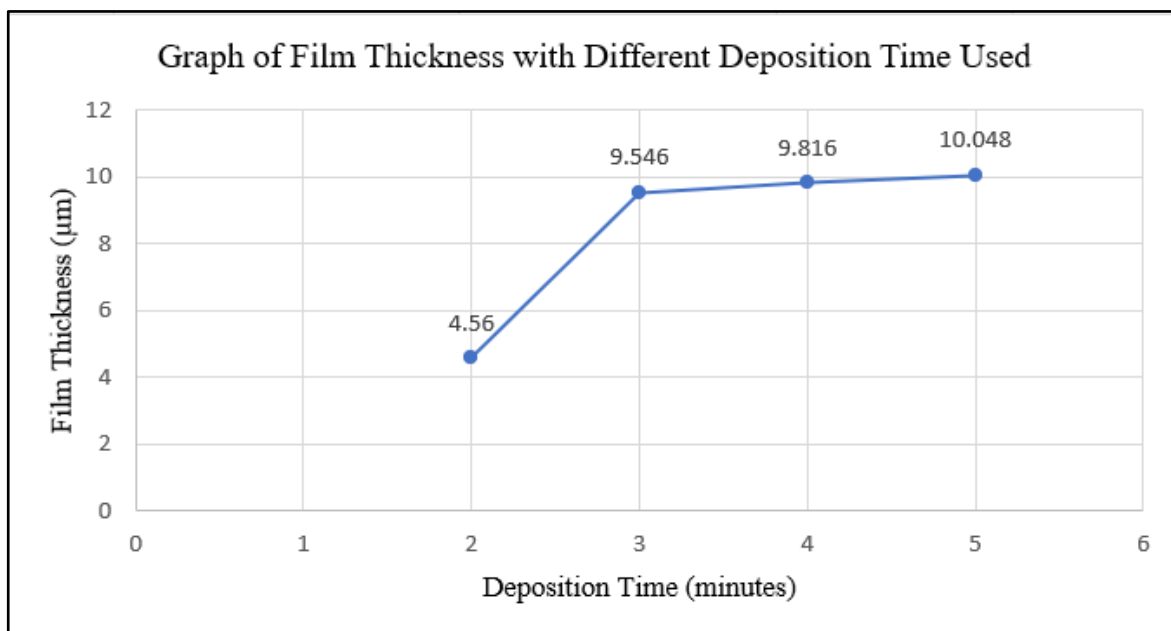


Figure 4.1 Thickness of MoSe₂ thin film with deposition time

Figure 4.1 shows the thickness variation with deposition time of a MoSe₂ thin film deposited on an ITO-coated glass substrate. The graph shows that the trend of film thickness grows as the deposition time increases from 10 minutes to 30 minutes. Initially, the thickness of the MoSe₂ thin film for a 10 minutes deposition time is 4.560 µm, indicating a very thin enough film and an incomplete electrodeposition procedure. The thin films are considered well deposited on the substrate and have uniform and good adhesion after 20 minutes. At 25 and 30 minutes, the thickness thickens and tends to be over-deposited.

4.3 XRD Structural Analysis

Figure 4.2 shows X-ray diffraction (XRD) patterns of an electrodeposited Molybdenum diselenide (MoSe₂) thin layer on a stainless-steel substrate. This method is used to analyse several relevant elements such as phase existing, phase density, crystalline type, and crystalline size or strain. Since glass substrate is a transparent material that is amorphous solid, thin films deposited on it are not studied when XRD measurements are performed on it. As a result, stainless steel substrate is used.

Table 4.2 XRD comparison of standard JCPDS values with experimental MoSe₂ values

Angle (2θ)	(h k l)	Standard (Å)	Experimental (Å)			
		'd' JCPDS	10 min	20 min	25 min	30min
12.23	0 0 3	6.460	7.23631	6.93607		
23.35	1 0 0	3.770			3.80936	3.79556
29.02	1 0 1	3.010		3.07674	3.09253	3.06793
44.05	1 0 7	1.985	2.05591	2.06035	2.07251	2.06626
50.70	0 1 8	1.846	1.80059	1.80059	1.80073	1.80333
74.68	0 2 7	1.265	1.27096	1.27061	1.27090	1.27151
82.03	1 1 12	1.152	1.17476			

The diffractogram of Figure 4.2, MoSe₂ thin films deposited on stainless steel substrate determined from XRD measurement, shows a sharp peak, indicating that MoSe₂ thin films was found to be polycrystalline in hexagonal structure. (Huan Lin, 2021). The Joint Committee of Powder Diffraction Standards (JCPDS) document is used to identify the XRD peak and its pattern. According to Table 4.2, the standard values of *d* were chosen based on the experimental values of which exist in the same range. As a result, the peak angle element has been identified. Figure 4.2 represents the investigation of peaks from various deposition times. Within 30 minutes, the peaks are defined as planes of selenium (Se) with the reference of JCPS Card, No. 00-001-085 shows two peaks that indicated at (1 0 0) and (1 0 1) with $2\theta = 23.35^\circ$ and $2\theta = 29.02^\circ$, respectively. MoSe₂ peaks were obtained. MoSe₂ planes (0 0 3), (1 0 7), (0 1 8), (0 2 7) and (1 1 12) were found as peaks at $2\theta = 12.23^\circ$, 44.05° , 50.70° , 74.68° , and 82.03° .

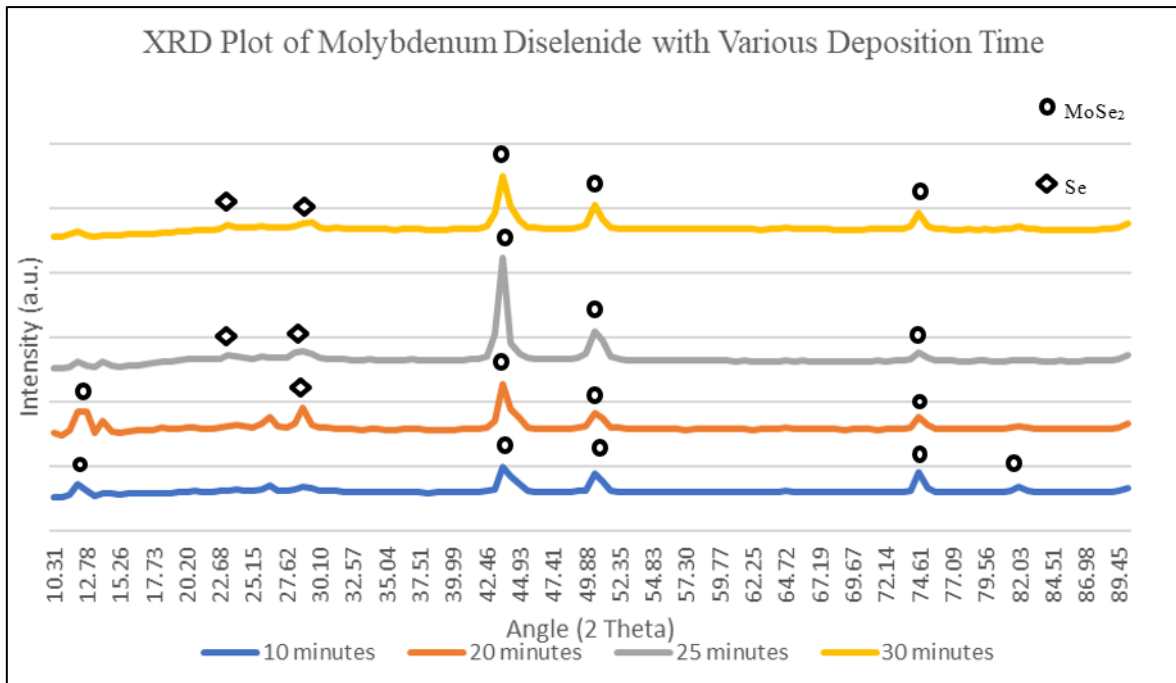


Figure 4.2 XRD pattern of MoSe₂ thin film at different deposition times

The peak of MoSe₂ at $2\theta = 44.05^\circ$, 50.70° becomes more significant as the deposition time increases, indicating that the (1 0 7) and (0 1 8) planes films grew with the deposition time. The deposition times of 10 minutes and 20 minutes are noted to be consistent and almost identical. The peak is observed to be different from other peaks from peaks of W at $2\theta = 12.23^\circ$, $2\theta = 29.02^\circ$, $2\theta = 44.05^\circ$ and $2\theta = 82.03^\circ$ at deposition time of 25 minutes and 30 minutes, respectively. This is due to the extended deposition time, which contributes to over-deposition and makes the deposit ununiform when compared to deposition times of 10 minutes, and 20 minutes. Peaks of MoSe₂ are almost similar at 10 minutes and 20 minutes deposition time before they continue to fluctuate for the next two deposition times. The (1 0 7) plane has a greater peak intensity and is the best plane orientation for the formation of MoSe₂ films. This indicates that the formation of polycrystalline structures that take place is consistent at 10 minutes and 20 minutes deposition times but not at 25 minutes, and 30 minutes deposition times. It is assumed that extending the deposition time will result in uneven crystalline growth.

According to JCPDS data, the lattice parameter value of MoSe₂ is $a = b = 3.2920\text{\AA}$ and $c = 19.3920\text{\AA}$, which has been reported to be hexagonal in structure and matches the lattice parameter determined from XRD measurement results. As a result of strong evidence from JCPDS data, Molybdenum diselenide thin films formed on the substrate can be classed as hexagonal crystal structure.

4.4 SEM Surface Morphological Analysis

Scanning Electron Microscope (SEM) is used to examine the surface morphology of MoSe₂ thin films on the substrate in order to determine surface uniformity. Table 4.3 shows the surface morphology of MoSe₂ thin films at various deposition times using magnifications of 3000x, 5000x, and 10000x to provide a more consistent view of the film's growth. The surface of the film is observed in the micrograph, and it can be seen in the state of uniform and the MoSe₂ thin coating completely covers the substrate's surface.

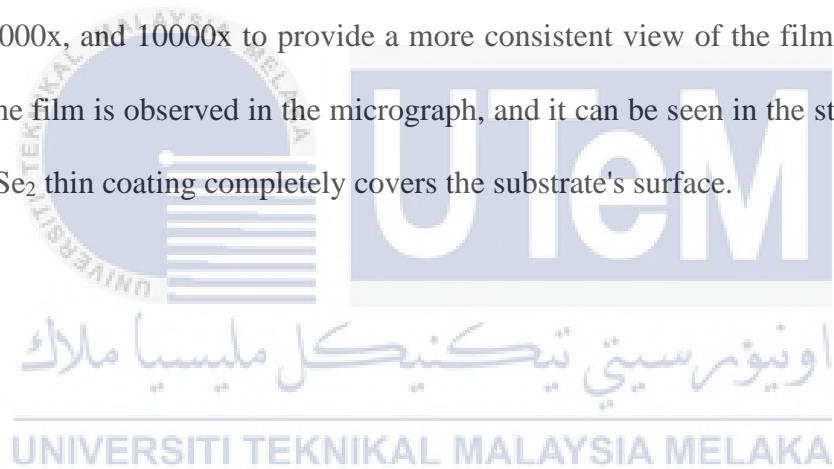


Table 4.3 SEM planar images of MoSe₂ films with different deposition times

Thin films deposition times	Magnification of SEM		
	3000×	5000×	10000×
10 minutes			
20 minutes			
25 minutes			
30 minutes			

The micrograph shows that MoSe₂ thin films started to form in the ion-ion growth phenomenon during the 10 minutes deposition time. Films are not well adherent to substrate in which an atom or molecules that develop on the substrate could be sulfur or molybdenum only. In comparison, thin films deposition time of 30 minutes have high adhesion of MoSe₂ with substrate. MoSe₂ thin films grew unevenly on the surface of substrate after 20 minutes

of deposition. The thin film has well adhered between substrate with the increasing of deposition time.

The surface morphology of the MoSe₂ film becomes piled up or thicker than the first two deposition times as the deposition times increase. This is due to MoSe₂ being over deposited as time increases. The pile up grain structure seems to form in an uneven structure during deposition times of 25 minutes and 30 minutes, which can cause pin-hole morphology to form on the surface. It can obstruct the interaction between the grains. As a result, the quality of the film will decrease. Knowledge of grain size and distribution is critical since the grain size governs the most significant properties of solar cells such as series and shunt resistances.

4.5 Optical Analysis

The optical characterization of Molybdenum diselenide (MoSe₂) thin films is investigated using a UV-Vis-NIR Spectrophotometer. The test is evaluated using the light absorbance spectrum from 200 nm to 1100 nm. The results are shown in Figure 4.3. The corresponding bandgap energy of MoSe₂ thin film was analysed using the transmittance spectrum and a Tauc plot of the films. The resultant plot has a straight line to the energy axis at x-axis that contributes to the onset of absorption. Thus, by extrapolating this linear region to an x-axis, one can determine the energy of the material's optical bandgap.

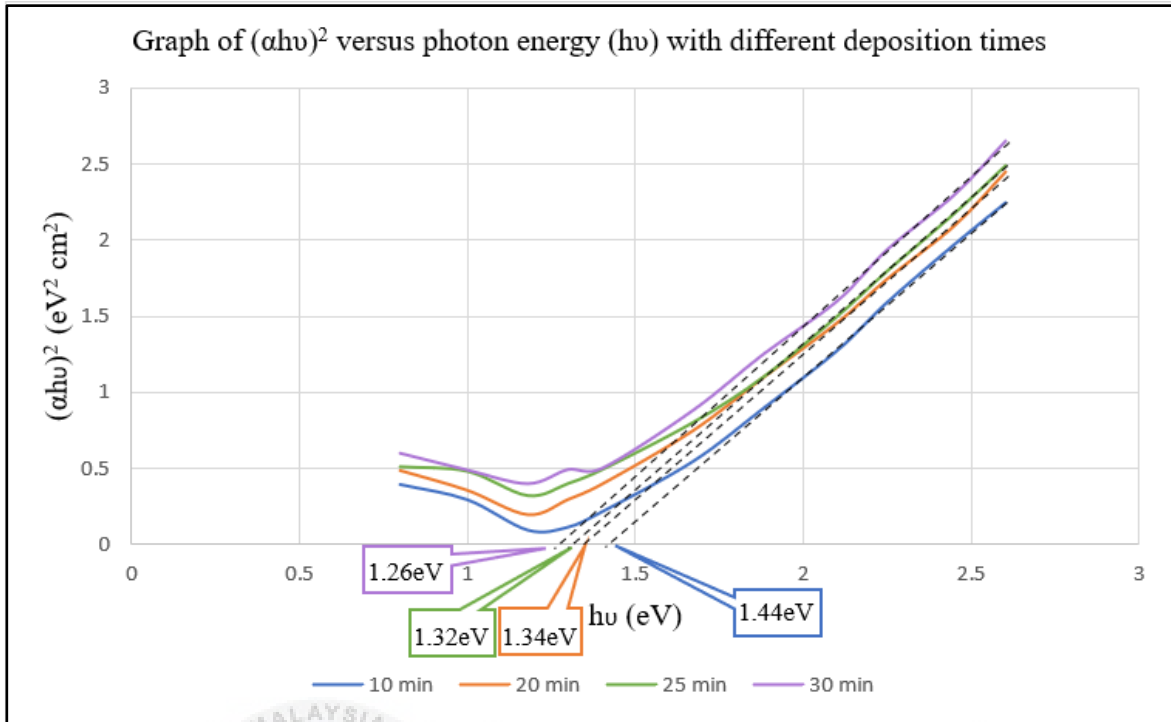


Figure 4.3 Graph of $(\alpha h\nu)^2$ versus photon energy ($h\nu$) with different deposition times

The optical transition in transition metal chalcogenides films is discovered to be direct and allowed type. As a result, the graph was drawn and the optical bandgap energy was determined by extrapolating the straight-line portion to cut the energy axis. The linear portion of the plot energy is more than 2 eV, which is a noticeable characteristic in the $(\alpha h\nu)^2$ vs. $h\nu$ plots. This indicates that the material is a direct transition type. Figure 4.3 shows the $(\alpha h\nu)^2$ vs. $h\nu$ plots of MoSe₂ thin films deposited at various deposition times. According to the figure above, energy bandgap of MoSe₂ thin films with different deposition times for 10 minutes, 20 minutes, 25 minutes and 30 minutes is determined which are 1.44 eV, 1.34 eV, 1.32 eV and 1.26 eV respectively.

Figure 4.4 represents the variation of bandgap energy (E_g) with deposition time, which shows non-linear decrease. The bandgap energy of the film is seen to decrease with increasing deposition time. The reported bandgap value of MoSe₂ thin films with various deposition times for 10 minutes, 20 minutes, 25 minutes, and 30 minutes is determined from

Figure 4.4 and is 1.44 eV, 1.34 eV, 1.32 eV and 1.26 eV respectively and this bandgap energy within a reasonable range with reported value of MoSe₂ by M.M. Vora *et al.* and A.M. Vora *et al.* (2008).

It could be determined that the optical bandgap energy of thin films decreases with increasing deposition time. This result relates to thickness of film, with higher deposition times resulting in thicker films.

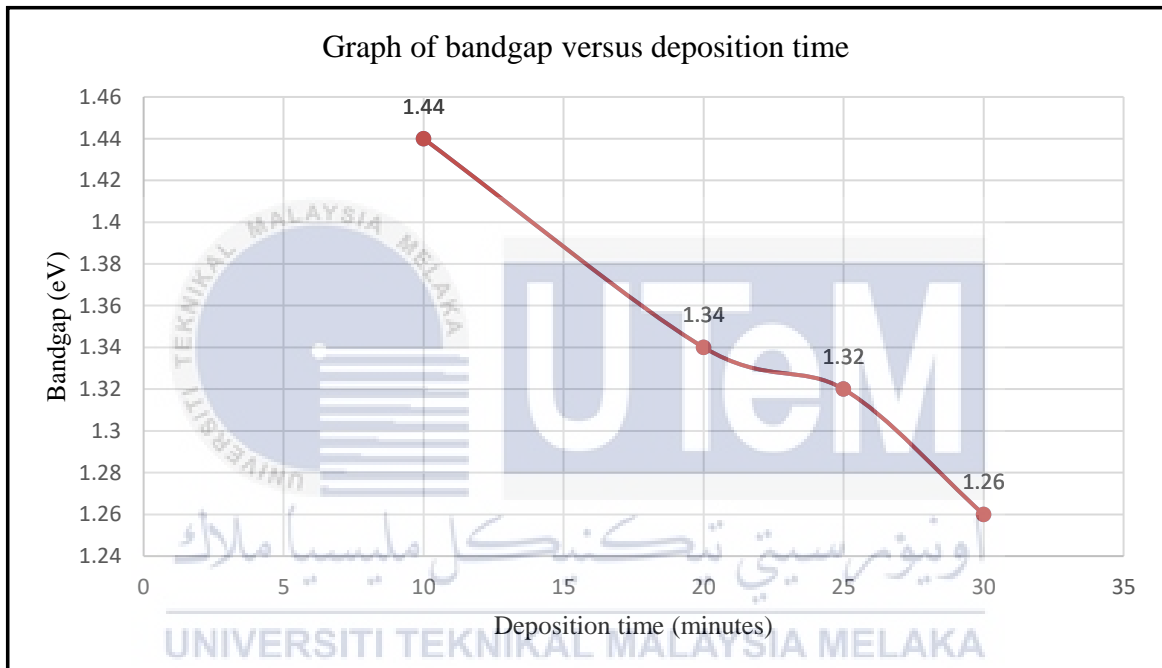


Figure 4.4 Graph of bandgap versus deposition time

4.6 Mott-Schottky Analysis

For the study of the semiconductor parameters, Mott-Schottky graphs have been drawn. The space-charge capacitance was measured using an LCR bridge meter and the Mott-Schottky graphs were then drawn using the capacitance data. It is created by plotting space charge capacitance versus the applied potential (V_{SCE}). The graph of the Mott-Schottky plot of MoSe₂ thin films with various deposition times is shown in Figure 4.5. Table 4.4 provides an overview of the semiconducting properties. As shown in Figure 4.5, the intersections of plots on the voltage axis determine the flat band potential value of the

junction. As the deposition time increases, the flat band potential (V_{fb}) value decreases from 0.87 V to 0.76 V. The V_{fb} value is important for solar cell applications because it determines the maximum feasible cell photovoltage.

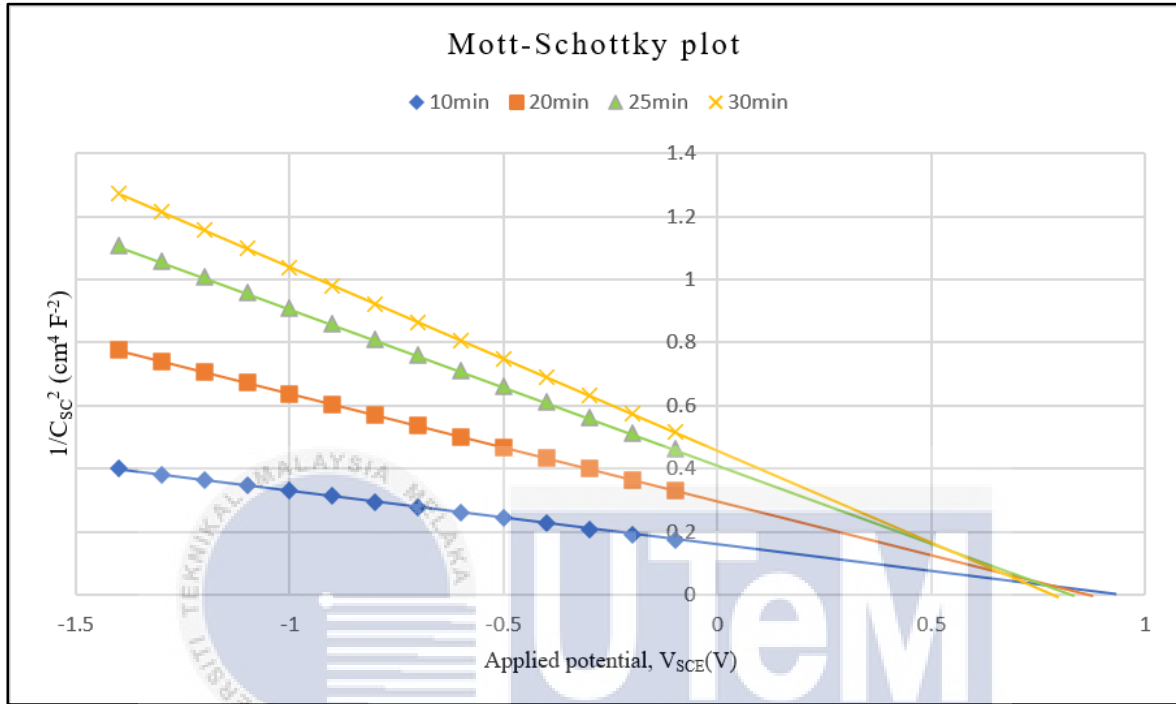


Figure 4.5 Mott-Schottky plot for MoSe₂ thin films at different deposition time

The flat band potentials, V_{fb} , of the junction are shown in the graphs of $1/C_{sc}^2$ against V_{SCE} , interception on the voltage axis. Flat band potentials, V_{fb} , rapidly decrease as deposition time increases. This is explained by Anand *et al.* (2012), who stated that the crystallinity of films increases as their thickness increases. The results of V_{fb} for 30 minutes deposition times are found to be in good agreement with the values reported in the Anand *et al.* (2012) study on the photoelectrochemical response of MoSe₂.

The figure's negative slope implies that MoSe₂ thin films are p-type semiconducting materials. As deposition time increases, the value of depletion layer width, W (Å) decreases, which is similar to the values of energy bandgap determined by optical analysis. The values of band bending, V_b , obtained from the literature review (Anand *et al.*, 2012). The dielectric

constant, ϵ values are in good agreement with those reported by Anand *et al.* (2012) for MoSe₂ thin films. Table 4.4 shows the data value. The dielectric constants of the films are also observed to decrease as the thickness of the films increases. Although the dielectric constant of MoSe₂ thin films decreases with time, this is a positive trend because a higher dielectric constant is not really desired. Substances with high dielectric constants often degrade faster when exposed to strong electric fields than those with low dielectric constants (Anand *et al.*, 2012).

In conclusion, the semiconducting characteristics of Molybdenum diselenide (MoSe₂) thin films obtained using Mott-Schottky plots are compared with those of other transition metal dichalcogenides, and the results show that the semiconducting parameters of MoSe₂ thin films are reasonable. As a result, MoSe₂ thin films can be established as an appropriate material for solar panels.

Table 4.4 Summary of results obtained from Mott-Schottky plots for MoSe₂

Semiconducting Parameters	Results			
	10 minutes	20 minutes	25 minutes	30 minutes
Type of semiconductor	p	p	p	p
Flat band potential, V_{fb} (V)	0.87	0.84	0.81	0.76
Band bending, V_b (V)	-0.575	-0.445	-0.345	-0.255
Dielectric constant, (ϵ)	44.1	37.3	34.1	33.5
Doping density, $N_D \times 10^{29}$ (m ⁻³)	1.83	1.10	0.83	0.72
Depletion layer width, W (Å)	2.98	1.94	1.49	1.24
Energy gap, E_g (eV)	1.44	1.34	1.32	1.26
Maximum conversion efficiency, η_{max}	6.40	5.32	4.19	3.24

CHAPTER 5

CONCLUSION AND RECOMMENDATIONS

5.1 Conclusion

This chapter provides the research's conclusions, recommendations, and sustainable elements. Conclusions are reached based on the study's goals and findings, and recommendations for resolving the problem that this research encountered are presented. Project potential show how this research can further be used and has impacted a number of related fields.

According to the previous results, it is approved to produce stoichiometric Molybdenum diselenide (MoSe_2) thin films using the electrodeposition method based on objective one. The ITO-coated glass substrate was successfully deposited in MoSe_2 thin film. Additionally, the fact that the deposition procedure continues even as the deposition time increases may be seen. In all of the various times of the deposition process, the stoichiometric still may be identified.

The XRD structural study of the thin film using the MoSe_2 thin film can be clarified as a polycrystalline structure with crystals that are hexagonal. With longer deposition times and thicker films, the XRD peaks for thin films become more intense. With regard to the surface morphology of the MoSe_2 thin film, which was examined using a scanning electron microscope (SEM), the micrograph shows that the lengthening of the deposition time is causing an uneven structure, which may affect the quality of the thin films and result in less effective performance from developing future appliances. The optical characteristics of MoSe_2 thin films with various deposition times show the direct bandgap and the energy

bandgap ranges from 1.44 eV to 1.26 eV, which is compatible with and required for a suitable semiconducting material.

In conclusion, all of the results for the semiconductor parameters of MoSe₂ thin films are investigated and p-type semiconductor material is seen to be present in the thin films. The value of the depletion layer width shows a decreasing trend, which complies with the requirements for a good semiconductor material, and the flat band potentials are decreased as a result of the growth of crystalline as the deposition time increases. As a result, thin films of Molybdenum diselenide (MoSe₂) can be categorised as appropriate semiconductor for solar panels.

5.2 Recommendations

Heat treatment, such as annealing, could be used to remove the oxygen content that adheres to the surface of the ITO coated glass substrate. The presence of oxygen has an effect on the stoichiometry of the MoSe₂ thin film. The oxygen can form a combination with molybdenum or selenium, influencing the stoichiometry of the MoSe₂ thin film. As a result, in order to obtain the stoichiometry MoSe₂ thin film, the oxygen content must be eliminated by annealing the previously deposited layer. Annealing treatment can improve thin film surface uniformity and crystallinity that improved transmittance. The crystallinity of the film improved significantly when the annealing temperature was increased. The increased crystallinity is thought to be related to greater energy provided to the film in terms of temperature, and it could cause less defects (Parashurama Salunkhe & Dhananjaya Kekuda, 2022), which can improve thin film characteristics for solar panel applications.

It is possible to look at the deposition's condition for future research. The results of the MoSe₂ thin film's stoichiometry can be impacted by the deposition's time and

temperature. It is simple to achieve the MoSe₂ thin film's stoichiometry by using the proper time and temperature for deposition of the film.

According to the analytical method, Transmission Electron Microscope (TEM) analysis need to be used instead of the current Scanning Electron Microscope (SEM) analysis to characterise the surface morphology of MoSe₂ thin films with atomic scale resolution and higher magnification micrograph. By comparing the transmitted and diffracted electron intensities, TEM can provide additional details about the films' characteristics, including their morphology, local structure, and chemistry of the transition metal dichalcogenides (TMDs) material.

5.3 Project Potential

In contrast to fossil fuels and natural gas, which have recently taken control of the energy sources and create significant environmental damage, solar energy is free and available in enormous numbers. Furthermore, solar energy requires significantly less manpower than traditional energy production techniques (Mohd Rizwan Sirajuddin Shaikh, 2017). Since sunlight is inexhaustible, solar energy is a renewable resource that won't run out in the future. Solar energy is a renewable energy source that may be used to replace current non-renewable energy sources and reduce environmental damage. Therefore, in the current state of solar cell research and development, thin films for solar cells are the most critical concern.

However, silicon is currently the most expensive semiconducting material for solar panels because to its high manufacturing complexity and alignment requirements. Then, due to the fact that transition metal dichalcogenides (TMDs) such as such as Cadmium, Tungsten and Nickel are candidates for absorbed layer in solar cells thin films due to their absorption

coefficient and energy band gap, research has focused on using TMDs as a replacement for silicon material in new generation photoelectrochemical cells (Wu. L, 2019).

Last but not least, TMDs thin films will be the solar panel candidates for now and in the future due to their simplicity of production and cheaper cost compared to silicon wafer preparation for solar panels.



REFERENCES

A.A. Yadav and E.U. Masumdar, 2010. Photoelectrochemical performances of n-CdS_{1-x}Se_x thin films prepared by spray pyrolysis technique. *Solar Energy*, vol. 84, Issue 8, pp. 1445-1452.

A. Brent Youn, 2006. *Plastics: Materials and Processing (Third Edition)*, Pearson, NJ.

Ajalkar B. D., Burungale S. H., Bhangre D. S., Bhosale P. N., 2004. Chemical synthesis and compositional analysis of mixed [Mo(S_{1-x}Se_x)₂] semiconductor thin films. *Journal of Materials Science*. 39, pp. 1659-1664.

Akhtar M., 2013. Synthesis of Iron Chalcogenide Nanocrystals and Deposition of Thin Films. Single Source Precursors. *PhD Thesis*. University of Manchester, UK.

Ali Hussain Reshak and Sushil Auluck, 2005. Band structure and optical response of 2H-MoX₂ compounds (X=S, Se, and Te). *Phys. Rev, Chemical Sciences*, vol.71, Issue 15, pp. 6.

Amelia Carolina Sparavigna, 2014. Light-Emitting Diodes in the Solid-State Lighting Systems. *International Journal of Sciences*, vol. 3, pp.9-17.

Aryan, N.P., H. Kaim and A. Rothermal, 2014. Stimulation and Recording Electrodes for Neural Prostheses. 1st Edn., Springer, Cham, Switzerland, pp. 79.

A.R. West, 2003. 'Solid State Chemistry'. John Willey & Sons, Singapore.

Ayotunde Adigun Ojo and Imyhamy Mudi Dharmadasa, 2018. Electroplating of Semiconductor Materials for Applications in Large Area Electronics: A Review. *Coatings*, 8, pp. 262.

Binwen Chen., Guilin Chen., Weihuang Wang., Huiling Cai., Liquan Yao., Shuiyuan Chen and Zhigao Huang, 2018. Magnetron sputtering deposition of GeSe thin films for solar cells. *Solar Energy*, 176, pp. 98-103.

B. Rameshkumar, A. Anderson, D. Ananth and T. Mohan, 2020. An investigation of SnO₂ nanofilm for solar cell application by spin coating technique. *AIP Conference Proceedings*, pp. 2341.

Britnell, L. *et al.*, 2013. Strong light-matter interactions in heterostructures of atomically thin films. *Science* 340, pp. 1311-1314.

B Weckhuysen, Pascal Van Der Voort (Ugent) And G Catana, 2000. Spectroscopy of Transition Metal Ions on Surfaces. Leuven University Press, pp. 308.

Canan Acar, Ibrahim Dincer, 2018. Energetic and exergetic investigations of an innovative light-based hydrogen production reactor. *International Journal of Hydrogen Energy*, vol. 43, Issue 22, pp. 10249-10257.

Choy, K.L., 2003. Chemical Vapour Deposition of Coatings. *Progress in Materials Science*, 48, pp. 57-170.

C. Lokhande, B. Sankapal, R. Mane, H. Pathan, M. Muller, M. Giersig, V. Ganesan, 2002. XRD, SEM, AFM, HRTEM, EDAX and RBS studies of chemically deposited Sb₂S₃ and Sb₂Se₃ thin films. *Materials Science, Applied Surface Science* 193, Issues 1-4, pp.1-10.

C. Rameshkumara, A. Andersonb, D. Anantha, T. Hinduja Mohanc and R.Subalakshmi, 2021. An investigation of SnO₂ nanofilm for solar cell application by spin coating technique. *Materials Today: Proceedings*, vol. 45, Part 7, pp. 6042-6045.

Damm, D.D., Contin, A., Barbieri, F.C., Trava-Airoldi, V.J., Barquete, D.M., Corat, E.J., 2017. Interlayers applied to CVD diamond deposition on steel substrate: A review. *Coatings*, 7, pp. 141.

David Tavakoli, 2020. X-Ray Diffraction (XRD) for the Analysis of Thin Films. Southeastern Nanotechnology Infrastructure Corridor.

Diego Martínez-Martínez, Carmelo Herdes, Lourdes F. Vega, 2017. Crystallization processes in bi-component thin film depositions: towards a realistic Kinetic Monte-Carlo simulation. *Surface & Coatings Technology*, 343, pp. 11.

Dmitri V Talapin, Elena V Shevchenko, Christopher B Murray, Andreas Kornowski, Stephan Förster, Horst Weller, 2004. CdSe and CdSe/CdS nanorod solids. *Journal of the American Chemical Society*, vol. 126, Issue 40, pp. 12984-12988.

Doroody, C., Rahman, K. S., Abdullah, S. F., Harif, M. N., Rosly, H. N., Tiong, S. K., Amin, N., 2020. Temperature difference in close-spaced sublimation (CSS) growth of CdTe thin film on ultra-thin glass substrate. *Results in Physics*, 18, pp. 103213.

Dr. Tapanendu Kamilya, 2020. Characterization: X-Ray Diffraction, Optical Microscopy, Scanning Electron Microscopy, Transmission Electron Microscopy, Atomic Force Microscopy, Scanning Tunnelling Microscopy. Physics (UG) Semester-VI Paper: DSE3T (Nanomaterials & Applications) 2.

Fabiana Lisco, Piotr Kaminski, Ali AbbasAli Abbas, Kevin BassKevin Bass, Jake BowersJake Bowers, Gianfranco ClaudioGianfranco Claudio, Maria Losurdo and Michael Walls, 2015. The structural properties of CdS deposited by chemical bath deposition and pulsed direct current magnetron sputtering. *Thin Solid Films*, 582, pp. 323 - 327.

Farzad Nasirpouri, 2016. Electrodeposition of nanostructured materials. Cham, Switzerland, Springer, vol. 62, pp. 325.

Freiburg, 2022. Photovoltaics Report. Fraunhofer Institute for Solar Energy Systems, ISE with support of PSE Projects GmbH.

Fultz, B. and Howe, J., 2013. Diffraction and the X-Ray Powder Diffractometer. Transmission Electron Microscopy and Diffractometry of Materials, Springer, pp. 1-57.

Goldstein J, Newbury D, Joy D, Lyman C, Echlin P, Lifshin E, Sawyer L and Michael J, 2007. Scanning electron microscopy and X-ray microanalysis. (Boston, MA: Springer)

Guma, T. N., Madakson, P. B., Yawas, D. S., Aku, S. Y., 2012. X-ray Diffraction Analysis of the Microscopies of Some Corrosion Protective Bitumen Coatings. *Int. J. Mod. Eng. Res.*, 2, pp. 4387–4395.

Haris Mehmood and T. Tauqeer, 2017. Modeling and performance analysis of amorphous silicon solar cell using wide band gap nc-Si: H window layer. *IET Circuits, Devices and Systems* 11, 6, pp. 666-675.

Haynes, William M., ed. (2011). CRC Handbook of Chemistry and Physics (92nd ed.). Boca Raton, FL: CRC Press. p. 4.76.

Hideaki Adachi and Kiyotaka Wasa, 2012. Thin Films and Nanomaterials. Handbook of Sputtering Technology (Second Edition), pp. 3-39.

Huan Lin, Ridong Wang, Hamidreza Zobeiri, Tianyu Wang, Shen Xu and Xinwei Wang, 2021. The in-plane structure domain size of nm-thick MoSe₂ uncovered by low-momentum phonon scattering. *Nanoscale*, 13, pp. 7723-7734.

J. A. Wilson and A. D. Yoffe, 1969. “The transition metal dichalcogenides discussion and interpretation of the observed optical, electrical and structural properties”. *Adv. Phys*, 18, pp. 193.

Karina Torres-Rivero, Clara Pérez-Ràfols, Julio Bastos-Arrieta, Núria Serrano, Vicenç Martí and Antonio Florido, 2021. Customized Screen-Printed Electrodes Based on Ag-Nanoseeds for Enhanced Electroanalytical Response towards Cd(II), Pb(II) and As(V) in Aqueous Samples. *Chem. Proc*, vol. 5, No. 1, pp. 87.

Kazi Sajedur Rahman, Muhammad Najib Harif, Hasrul Nisham Rosly, Mohamad Ibrahim Bin Kamaruzzaman, Md.Akhtaruzzam, Mohammad Alghoul, Halina Misran, Nowshad

Amin, 2019. Influence of Deposition Time in CdTe Thin Film Properties Grown by Close-Spaced Sublimation (CSS) for Photovoltaic Application. *Results in Physics*, vol. 14, pp. 102371.

K.N. Nithyayini and Sheela K. Ramasesha, 2015. Fabrication of Semi-Transparent Photovoltaic Cell by a Cost-Effective Technique. *Metallurgical and Materials Transactions*, vol. 2E, 3, pp. 161.

Kumar, V., S. Kalia and H.C. Swart, 2016. Conducting Polymer Hybrids. Springer, Berlin, Germany, pp.335.

K. W. Mitchell, Margorie L. Tatro, 2017. Solar cell. AccessScience from McGraw-Hill Education.

Lai, Y. Q., Liu, F. Y., Zhang, Z. A, Liu, J.,Li, Y., Kuang, S. S., Liu J., Liu Y. X., 2009. "Cyclic voltammetry study of electrodeposition of Cu(In,Ga)Se₂ thin films". *Electrochimica Acta*, vol. 54(11), pp. 3004-3010.

Lamas, D.G., Neto, M.D.O., Kellermann, G., Craievich, A.F., 2017. X-ray Diffraction and Scattering by Nanomaterials. In *Nanocharacterization Techniques*; William Andrew Publishing: Oxford, UK, Chapter 5, pp. 111-182.

Lee, H., Kim, H., Lee, J., Kwak, J., 2019. Fabrication of a Conjugated Fluoropolymer Film Using One-Step iCVD. Process and its Mechanical Durability. *Coatings*, vol. 9, No. 7, pp. 430.

Lincot, D., J. F. Guillemoles, S. Taunier, D. Guimard, J. Sicx-Kurdi, A. Chaumont, O. Roussel, O. Ramdani, C. Hubert, J. P. Fauvarque, N. Bodereau, L. Parissi, P. Panheleux, P. Fanouillere, N. Naghavi, P. P. Grand, M. Benfarah, P. Mogensen and O. Kerrec, 2004. "Chalcopyrite thin film solar cells by electrodeposition." *Solar Energy* 77(6), pp. 725-737.

Lucio Claudio Andreani, 2018. Silicon solar cells: Toward the efficiency limits. *Advances In Physics: X*, vol. 4, No. 1, pp. 1548305.

Lu, J. *et al.*, 2017. Exfoliated nanosheet crystallite of cesium tungstate with 2D pyrochlore structure: synthesis, characterization, and photochromic properties. *ACS Nano*, 11, pp. 1689–1695.

Luo, Run, Liu, B., Yang, Xiaoyan, Bao, Zheng, Li, Bing, Zhang, Jingqua, Li, Wei, Wu, Lili, Feng, Lianghuan, 2016. The Large-Area CdTe Thin Film for CdS/CdTe Solar Cell Prepared by Physical Vapor Deposition in Medium Pressure. *Applied Surface Science, Elsevier B.V.*, 360, pp. 744-748.

Martin-Litas, I. *et al.*, 2002. Characterisation of r.f. sputtered tungsten disulfide and oxysulfide thin films. *Thin Solid Films*, vol. 416, Issues 1-2, pp. 1–9.

Micheal Hart, 1981. Bragg angle measurement and mapping. *Journal of Crystal Growth*, vol. 55, Issue 2, pp. 409-427.

M.M. Vora, A.M. Vora, 2008. Stacking faults in Re doped MoSe₂ single crystals, *Chalcogenide Letters*, vol. 5, pp. 35-37.

Mohd Rizwan Sirajuddin Shaikh, 2017. A Review Paper on Electricity Generation from Solar Energy. *International Journal for Research in Applied Science & Engineering Technology (IJRASET)*. Volume 5, Issue IX, pp. 184.

Murai, S., Sato, T., Yao, S., Kmakura, R., Fujita, K. and Tanaka, K. (2016) 'Fabrication of cerium-doped yttrium aluminum garnet thin films by a mist CVD method', *Journal of Luminescence*, Elsevier, 170, pp.808-811.

Naba R. Paudel and Yanfa Yan, 2014. Enhancing the photo-currents of CdTe thin-film solar cells in both short and long wavelength regions. *Applied Physics Letters* 105, 183510.

N Pappas, 2006. Calculating retained austenite in steel post magnetic processing using X-ray diffraction. *B S Undergrad Maths. Exchange*, 4(1), pp. 8–14.

Nutan S. Satpute S.J. Dhoble, 2021. Chapter 14 - Role of rare-earth ions for energy-saving LED lighting devices. *Energy Materials, Fundamentals to Applications 2021*, pp. 407-444.

Parashurama Salunkhe & Dhananjaya Kekuda, 2022. Effect of annealing temperature on the physical properties of NiO thin films and ITO/NiO/Al Schottky diodes. *Journal of Materials Science: Materials in Electronics* volume 33, pages 21060–21074 (2022).

Paul Fewster, 1999. Absolute Lattice-Parameter Measurement. *Journal of Materials Science: Materials in Electronics*, vol. 10, No. 3, pp. 175-183.

PMP Salomé, Jan Keller, Tobias Törndahl, JP Teixeira, N Nicoara, R-Ribeiro Andrade, DG Stroppa, JC González, Marika Edoff, JP Leitão, S Sadewasser, 2017. CdS and $Zn_{1-x}Sn_xO_y$ buffer layers for CIGS solar cells. *Solar Energy Materials and Solar Cells*, 159, pp. 272-281.

Rahaman, M.Z and Akther Hossain, A.K.M., 2018. Effect of metal doping on the visible light absorption, electronic structure and mechanical properties of non-toxic metal halide $CsGeCl_3$. *RSC Adv*, 8, pp. 33010–33018.

Rahman Kazi Sajedur, *et al.*, 2019. Influence of deposition time in CdTe thin film properties grown by Close-Spaced Sublimation (CSS) for photovoltaic application. *Journal of ScienceDirect, Results in Physics*, vol. 14, pp. 102371.

Roy P, Srivastava SK, 2006. Chemical bath deposition of MoS_2 thin film using ammonium tetrathiomolybdate as a single source for molybdenum and sulphur. *Thin Solid Films* 496, pp. 293.

R.S.Mane and C.D.Lokhande, 2000. Chemical deposition method for metal chalcogenide thin films. *Materials Chemistry and Physics*, vol. 65, Issue 1, pp. 1-31.

Simya O.K, P. Radhakrishnan Nair, Anuradha M Ashok, 2018. Chapter 41-Engineered nanomaterials for energy applications- "Nanomaterials for Solar Energy Generation" In book: Handbook of Nanomaterials for Industrial Applications, pp.751-767.

Sjöström, J.K., Bindler, R., Granberg, T., Kylander, M.E., 2019. Procedure for Organic Matter Removal from Peat Samples for XRD Mineral Analysis. *Wetlands*, 39, pp. 473–481.

S. Shariza and T. Joseph Sahaya Anand, 2012. A study on molybdenum sulphoselenide ($\text{MoS}_x\text{Se}_{2-x}$, $0 \leq x \leq 2$) thin films: Growth from solution and its properties. *Electrochimica Acta*, vol. 81, pp. 64–73.

S. Shariza and T. Joseph Sahaya Anand, 2011. Effect of Deposition Time on The Structural and Optical Properties of Molybdenum Chalcogenides Thin Films. *Chalcogenide Letters*, vol. 8, No. 9, pp. 529–539.

S. Shariza and T. Joseph Sahaya Anand, 2018. Structural and Optical Properties of Nickel Sulfoselenide (NiSSe) Thin Film for Photoelectrochemical Applications. *Journal of Science and Technology*, vol. 10, No. 2, pp. 53-60.

Sheet, S.D. (2013) 'Hydrochloric Acid, 50% v/v Hydrochloric Acid, 50% v/v Safety Data Sheet', 77(58), pp.1-7.

Stokes, Debbie J., 2008. Principles and Practice of Variable Pressure Environmental Scanning Electron Microscopy (VP-ESEM). Chichester: John Wiley & Sons.

Subramanian, B., C. Sanjeeviraja and M. Jayachandran, 2003. Materials properties of electrodeposited $\text{SnS}_{0.5}\text{Se}_{0.5}$ films and characterization of photoelectrochemical solar cells. *Materials Research Bulletin*, 38, pp. 899-908.

Taoufik Slimani Tlemçani, El Bachir Benamar, Fouzia Cherkaoui El Moursli, Faiza Hajji, Zineb Edfouf, Mhamed Taibi, Hicham Labrim, Bouchra Belhorma, Safae Aazou, Guy Schmerber, Karima Bouras, Zouheir Sekkat, Aziz Dinia, Alexander Ulyashin, Abdelilah Slaouif and Mohammed Abd-Lefdil, 2015. Deposition Time Effect on the Physical Properties of $\text{Cu}_2\text{ZnSnS}_4$ (CZTS) Thin Films Obtained by Electrodeposition Route onto Mo-coated Glass Substrate. *Energy Procedia* 84, pp.127 – 133.

Th. Böker, R. Severin, A. Müller, C. Janowitz, R. Manzke, D. Voß, P. Krüger, A. Mazur, and J. Pollmann, 2001. Band structure of MoS₂, MoSe₂, and α -MoTe₂: Angle-resolved photoelectron spectroscopy and ab initio calculations. *Phys. Rev.*, vol. 64, Issue 23.

Tiwari, A., Natarajan, S., Eds., 2017. Tribological Coatings. In *Applied Nanoindentation in Advanced Materials*; Wiley: New York, NY, USA, pp. 111–133.

T. Joseph Sahaya Anand, Rajes KM Rajan and Abdul Aziz Mohd Zaidan, 2013. Electrosynthesized NiS₂ thin films and their Optical and Semiconductor studies. *Reports in Electrochemistry*, vol. 3, pp. 25-29.

Trucchi, D.M., Bellucci, A., Girolami, M., Mastellone, M., Orlando, S., 2017. Surface texturing of CVD diamond assisted by ultra short laser pulses. *Coatings*, 7, pp. 185.

Vipin Kumar and D.K. Dwivedi, 2013. Study on structural, optical and electrical properties of CdS_{0.5}Se_{0.5} thin films for photovoltaic applications. *Optik - International Journal for Light and Electron Optics* 124(16), pp. 2345–2348.

Wu, L, 2019. Transition metal chalcogenide based functional materials for renewable energy conversion. [Phd Thesis I (Research TU/e / Graduation TU/e), Chemical Engineering and Chemistry]. Technische Universiteit Eindhoven.

Y. Deng, W. Chen, B. Li, C. Wang, T. Kuang, and Y. Li, 2020. Physical vapor deposition technology for coated cutting tools: A review. *Ceramics International*, vol. 46, no. 11, pp. 18373-18390.

Ying Zhuo, 2021. Investigation of nanostructured lithium-ion battery materials. Thesis for: Doctoral, Friedrich-Alexander-Universität Erlangen-Nürnberg (FAU).

Y. Gao, H. Niu and C. Q. Chen, 2003. Preparation and characterization of single-crystalline bismuth nanowires by a low-temperature solvothermal process. *Chem. Phys. Lett.* 367, pp. 141-144.

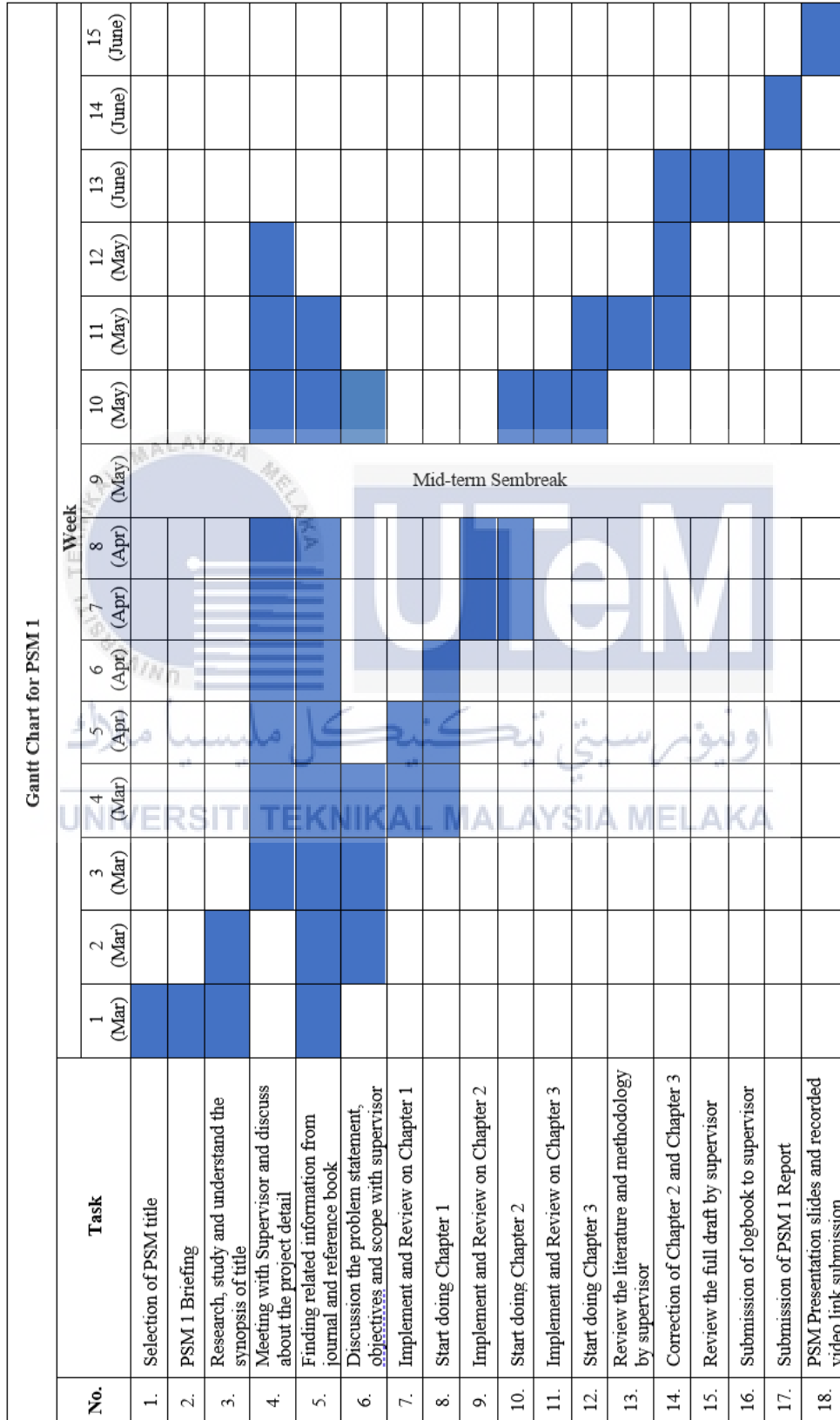
Zhang, Kaili, Li, Yahao, Deng, Shengjue, Shen, Shenghui, Zhang, Yan, Pan, Guoxiang, Xiong, Qinqin, Liu, Qi, Xia, Xinhui, Wang, Xiuli, Tu, Jiangping, 2019. Molybdenum Selenide Electrocatalysts for Electrochemical Hydrogen Evolution Reaction. *ChemElectroChem*, 6(14), pp. 3530-3548.

Zhou, H., Tao, F., Hiralal, P., Ahnood, A., Unalan, H. E., Nathan, A., and Amaratunga, G. A. J., 2014. Periodic nanopillar N-I-P amorphous Si photovoltaic cells using carbon nanotube scaffolds. *IEEE Transactions on Nanotechnology*, 13, pp. 997–1004.



APPENDICES

APPENDIX A Gantt Chart for PSM 1 (Semester 6, March, 2022)



APPENDIX B Gantt Chart for PSM 2 (Semester 8, October, 2022)

